

## TOPICAL REVIEW

# Fault Level Considerations in Tomorrow's Wind and PV-Rich Power Grids: A Review

RAFAT ALJARRAH<sup>1</sup>, (Member, IEEE), MAZAHER KARIMI<sup>2</sup>, (Senior Member, IEEE),  
AND HESAMODDIN MARZOOGHI<sup>3</sup>, (Member, IEEE)

<sup>1</sup>Electrical Engineering Department, Princess Sumaya University for Technology, Amman 1941, Jordan

<sup>2</sup>School of Technology and Innovations, University of Vaasa, 65200 Vaasa, Finland

<sup>3</sup>Strategic Network Solutions, Sydney, NSW 2010, Australia

Corresponding author: Mazaher Karimi (mazaher.karimi@uwasa.fi)

The work of Mazaher Karimi was supported by the InnoWind Project, co-funded by the European Union through the Just Transition Fund (JTF) and administered by the Regional Council of Ostrobothnia (Österbottens förbund).

**ABSTRACT** The increased penetration of Renewable Energy Sources (RESs), such as Photovoltaic (PV) and wind energy, in transmission and distribution networks is changing the features of current and future power systems. RESs may alter the characteristics of power systems due to their different dynamic behavior and limitations compared to centralized conventional Synchronous Generators (SGs). This is mainly attributed to Power Electronics (PE) interfaces (i.e., converters) utilized for integration with the power grid. As PE-based RESs exhibit lower and significantly different fault current contributions than SGs, fault level reduction is considered a major challenge for future power systems. Besides, such RESs may introduce new dynamics into the short-circuit (SC) current characteristics of power systems, which, in turn, may pose challenges to the strength, stability, operation, and protection of the grids. To tackle such challenges, it is essential to better understand the SC characteristics of the different RESs, specifically Wind and PV systems. In addition, evaluating their impact on the system fault level is necessary, especially in future power scenarios where most of the power is expected to be met by RESs. Hence, this study provides a comprehensive review of the contributions of SC currents from RESs to SC dynamics and the system fault level, addressing key challenges and gaps in the literature for researchers and utility engineers.

**INDEX TERMS** Photovoltaic, reduced fault level, renewable-rich power systems, renewable's fault contributions, system strength, wind energy.

## LIST OF ACRONYMS AND ABBREVIATIONS

RESs	Renewable Energy Sources.
PE	Power Electronics.
SGs	Synchronous Generators.
SC	Short Circuit.
TSOs	Transmission System Operators.
FRT	Fault Ride-Through.
LVRT	Low Voltage Ride-Through.
ENTSO-E	European Network of Transmission System Operators for Electricity.
$U_{ret}$	The connection point's retained voltage.
$T_{clear}$	The fault clearing time.
$U_{rec}$	The lower limit of voltage recovery.

$t_{rec}$	The time at the lower limit of voltage recovery.
Type-I	Squirrel-cage induction wind generator.
Type-II	Wound rotor induction wind generator with external rotor resistance.
Type-III	Doubly-fed asynchronous wind generator.
Type-IV	Full power converter wind generator.
Type V	Synchronous wind generator mechanically connected through a torque converter.
SCIG	Squirrel cage induction generator.
DFIG	Double-Fed Induction Generators.
VSC	Voltage Source Converter.
LCC	Line-Commutated Converters.
AEMO	Australian Energy Market Operator.
AEMC	Australian Energy Market Commission.
OCRs	Over Current Relays.
SCR	Short Circuit Ratio.

The associate editor coordinating the review of this manuscript and approving it for publication was Majdi Mansouri.

PLL Phase-Locked Loop.  
AVR Automatic Voltage Regulator.

## I. INTRODUCTION

The substantial integration of Renewable Energy Sources (RESs) is one of the distinguished characteristics of future power systems. In 2020, the total energy consumed globally from RESs was approximately 27,000 TWh, which represents around 17% of total energy consumption in the world. The endeavor to use more RESs is motivated by the increased demand, climate change, and the response to low carbon emissions strategies worldwide. Global figures show that most countries not only intend to meet their electrical demand from RESs, but also to move towards electrification of different sectors such as heating, cooling, transport, and industry. Such transition implies that more RESs should be integrated into the power grids, hence the operation of future power systems will be less dependent on traditional non-RESs generation. Fig. 1 shows the annual additions of renewable power capacity by technology between 2014-2020 where RESs (mainly PV and Wind) have shown a rapid increase among the other resources [1], [2], [3]. RESs have produced more than half of the additional power capacity added globally for power generation since 2012. In 2017, a remarkable new record of 167 GW (representing over 60%) was achieved for the global addition of newly built renewable power capacity [2]. This in turn allows the world not only to have secure energy, but also to possibly reverse global warming and to reduce the millions of air-pollution related death cases. Besides, it allows to produce low-cost energy and move towards achieving the zero-emission energy target [4]. Many countries and policymakers have started to pay attention to this issue in their regulations and have set a timeline for achieving energy transmission towards RESs as one of the important future goals. According to [5], renewable energy stood out as the sole electricity generation source to experience a net increase in overall power capacity in 2020, which established a record for new power capacity. Regardless of both social and political barriers that may be manifested, previous studies have pointed to the techno-economic feasibility of the transition towards 100% RESs worldwide [4], [6], [7].

As an example, a study conducted in [7] has laid out a comprehensive plan for all 50 states in the United States to transition their energy systems entirely to rely on Renewable Energy Sources (RESs). That plan has targeted replacing 85% and 100% of the current energy systems with RESs by 2030 and 2050, respectively. Furthermore, the G20 countries have set a collective goal of achieving an 85% share of RESs, with major contributions from China (26%), the United States (15%), India (12%), and the European Union (9%) [2]. Such a trend is usually accompanied by a displacement of conventional fossil fuel-based central synchronous generators (SGs).

All those figures and trends show that the future power grids would witness a very high share of RESs, mainly PV

and Wind. Regardless of the positive advantages that such RESs would add to the energy sectors globally [8], they might bring several key challenges [9], [10], [11]. As sources utilize Power Electronics (PE) interfaces (i.e., converters) for grid integration [12], the traditional dynamics of the power systems based on classical SGs, would be altered, and significantly affected by the dominated RESs [13]. The reduced fault level and the different characteristics of SC current dynamics are considered main aspects that would be highly possibly seen in future power systems more specially in RESs-dominated scenarios [14]. This is due to the limited and very different characteristics of the SC current contribution of the RESs when compared to the high and time-decaying SC contribution of large central SGs [15]. Accordingly, system strength, traditional protection systems, and system stability are potentially to be affected as a result of such new characteristics and altered dynamics [13], [16], [17]. Therefore, it is essential to understand the distinguished characteristics of such RESs, especially when it comes to their SC current contribution and their fault response to better characterize and quantify the consequences of the reduced fault level and the changed SC current dynamics in future power scenarios. This includes control, the Fault Ride Through (FRT) capabilities, and grid codes governing such RESs.

A wide range of literature can be found on the theme of SC current contribution of RESs, the FRT capability and grid codes requirements and the control of RESs [18], [19], [20], [21], [22], [23], [24], [25], [26], [27], [28], [29], [30]. While some of them have analyzed the SC contribution of some RESs like PV systems [19], [30], and some types of Wind generators specifically [20], [31], [32], [33], [34], [35], [36], [37], the other have provided a general insight on the fault current contribution of inverter-based sources and compared them to the ones fed by SGs [18], [21], [38], [39]. On the other hand, other studies have discussed the grid code requirements and the FRT control of different RESs [23], [29], [40], [41], [42], [43], [44], [45], [46], [47], [48], [49], [50].

Regarding the challenges associated with the potential very high share of RESs based on PV and Wind, a decent amount of literature can be also found [51], [52], [53], [54], [55], [56]. However, most of those studies have only focused on the frequency behavior and frequency control in low inertia systems. While a few studies can be found on the theme of system stability [57], [58], and protection challenges in future power systems with high penetration of RESs [10], [11], [36], few research have tackled the potential implications of reduced fault level and altered SC dynamics on the system strength and stability of RESs-rich power systems [59], [60], [61], [62], [63].

Even though there are several studies that cover different aspects of renewable-based systems, there is no single state-of-the-art review can be found that provides a solid comparison of the SC current response of PV and all types of wind generation in such a way to consider all the previously mentioned aspects collectively.

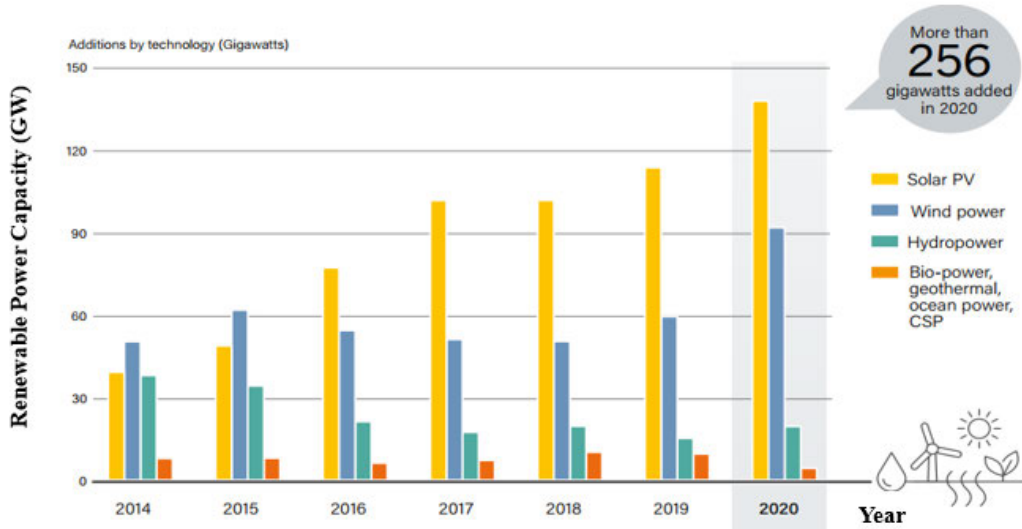


FIGURE 1. The annual additions of renewable power capacity by technology between 2014-2020 [3].

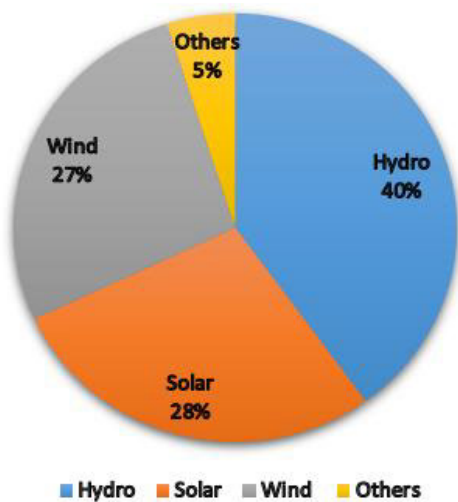


FIGURE 2. Global added RESs in percentage by 2021 [65].

Also, the body of current knowledge is still fragmented and lacks a cohesive technical viewpoint. Instead of synthesizing the SC current behavior, fault level evolution, system-strength implications, and grid-code requirements in an integrated manner for both PV and all wind generator types, current reviews usually concentrate on isolated topics—such as frequency stability, inverter control, or FRT compliance. This gap becomes increasingly critical as modern grids move toward high penetration of RESs, where the interplay between altered fault dynamics and grid strength is central to planning and operation. Therefore, a consolidated and comparative analysis is necessary to support researchers, system operators, and utilities in understanding the emerging challenges of RES-dominated power systems.

Hence, in order to fill this crucial gap, this paper offers a thorough and comparative analysis that concurrently looks at

the SC current characteristics of PV and all wind generation technologies, their changing FRT/grid-code requirements, and the resulting implications on system strength, protection performance, and overall stability in future RESs-dominated grids.

It is worth pointing that the review methodology employed in this study involved a systematic search using key terms such as “short-circuit current,” “fault level,” “photovoltaic,” “wind energy,” and “renewable energy sources”. Reputable databases, including IEEE Xplore, ScienceDirect, and Google Scholar, were used to ensure comprehensive coverage.

We prioritized peer-reviewed papers and technical reports published in the last 15 years, with a focus on studies addressing SC characteristics and fault levels in renewable-rich power systems. Selected papers were critically assessed for their contributions to understanding the impact of RESs on system dynamics, fault levels, system strength, and protection, ensuring a balanced and objective review. This structured methodology ensures the technical validity, completeness, and reproducibility of the presented review findings.

The subsequent sections of this paper are structured as follows: Section II outlines global figures and trends concerning RESs. In Section III, a comprehensive examination of the fault level concept within classical power systems is provided. Section IV undertakes an analysis of the progressive developments in grid codes and FRT requirements specific to PV and Wind RESs. Section V delves into an extensive exploration of the fault current contributions originating from PV and Wind Energy Sources. Subsequently, Section VI deliberates on the implications of the increased penetration of large-scale PV and Wind RESs on fault level, addressing potential adverse impacts on system strength, protection mechanisms, and system stability.

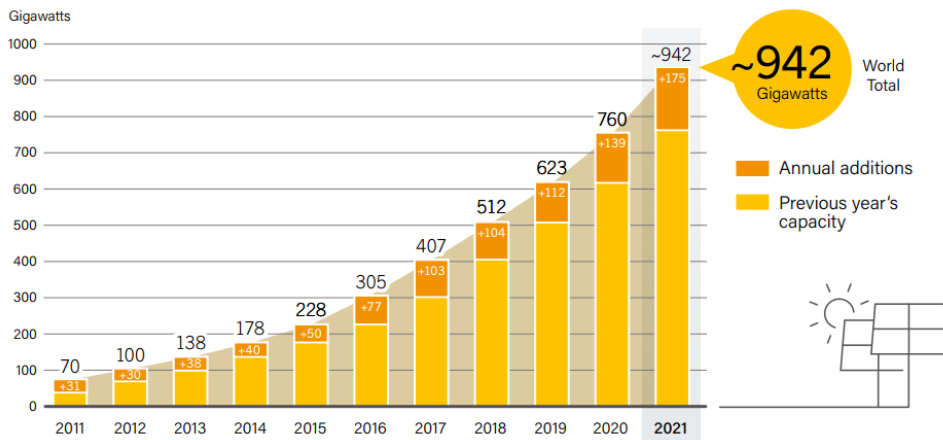


FIGURE 3. Solar PV global capacity and annual additions, 2011-2021 [65].

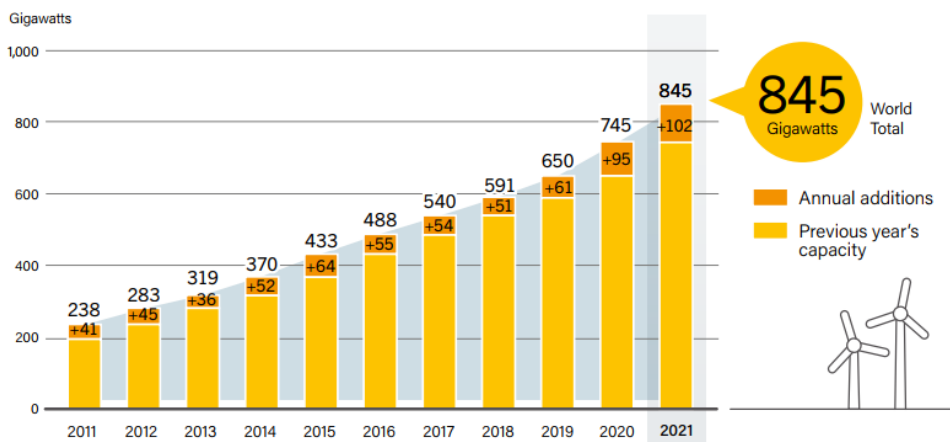


FIGURE 4. Wind Power Global Capacity and Annual Additions, 2011-2021 [65].

Finally, Section VII summarizes the paper with concluding remarks.

## II. GLOBAL FIGURES ON PV AND WIND SOURCES WORLDWIDE

Global figures and trends have shown a rapid movement towards RESs [64]. By the conclusion of 2021, the total global renewable generation capacity reached 3.064 TW. The most significant portion was attributed to hydropower, accounting for 1.230 TW of capacity. Solar and wind power equally shared the rest, with capacities of 942 GW and 845 GW, respectively. Other renewable sources comprised 524 MW of marine energy, 143 GW of bioenergy, and 16 GW of geothermal energy [65], [66], as shown in Fig. 2.

### A. PHOTOVOLTAIC SYSTEMS (PVS)

The electricity generated from PV sources is experiencing rapid growth, both in terms of absolute magnitude and as

a proportion of global generation. PV is expanding quickly and is playing a crucial part in the existing and future energy mix. In the last 20 years, the scale of deployed PV capacity has changed from kW to MW and then GW, and it is anticipated that the significant milestone of achieving 1 TW of installed global capacity will be reached within the next two years [67]. As an example, PV sources contributed to approximately 3.4% of the total global electricity energy generated in 2020. This represents five thousand times of the energy generated by PVs in 1990. Although this 3.4 % percentage seems small for the total global electricity energy generated, it is considered as a big transition compared to the 1.1% registered in 2015. These numbers indicate that the PV share has tripled in five years only. This transition in the amount of the PV share is attributed to the global awareness of the importance of the RESs, the increased efficiency of the manufactured PV modules, and the significant decline in the PV technologies price [68]. The ability to install PVs at the household scale has also contributed to the noticeable growth in the PV mar-

ket worldwide. Fig. 3, shows the solar PV global capacity and annual additions over the period between 2011-2021 [66].

### B. WIND ENERGY

Like solar PVs, wind energy is trending worldwide. The data indicates that around 94 GW of capacity had been installed globally in 2021, signifying the wind industry's second-best year on record, with a slight decrease of only 1.8% compared to the exceptional growth observed in 2020 [69], [70]. The statistics clearly demonstrate that 2021 marked the most successful year in offshore wind history, with an impressive 21.1 GW of offshore wind capacity commissioned. This amount is three times greater than what was installed in 2020, resulting in an increased market share of global new installations, reaching 22.5%. The yearly global trend of the wind installed capacity has shown a significant increased level, more specifically in the last decade. For instance, the added capacity has registered a value of 41 GW in 2011, while the maximum value of 95 GW has been added in 2020. The total global installed capacity has registered 283 GW and 745 GW for both years, respectively. This represents an increment of 263%, with a yearly increase of 26.3% approximately. It is worth noting that this has been varied according to the region/country. For instance, China added most of the newly installed wind capacity (46.9 GW) in 2021, followed by the US (14.0 GW).

In Europe alone, the wind has 236 GW of capacity, which accounted for more than 16% of the electricity consumed in 2020. While offshore wind energy has grown steadily over time, reaching about 7% of the world's wind capacity in 2021, it still makes up a minor portion of the industry. For instance, 81% of the new wind installations in Europe were onshore in 2020. During the same year, the Netherlands took the lead in installing the highest amount of wind power, primarily focusing on offshore installations. On the other hand, Norway led in onshore wind installations, with Spain and France following closely behind. However, the UK has installed most of the newly added wind (15%) as they accounted for most of the offshore installations in Europe in 2021. For onshore wind, Sweden came first with 12%, followed by Germany and Turkey with 11% and 8% in 2021, respectively [69]. Between the years 2022 and 2026, Europe is projected to construct 116 GW of new wind farms, resulting in an average of 23 GW annually. Fig. 4 displays the wind global capacity and annual additions over the period between 2011-2021 [66].

### III. FAULT LEVEL IN CLASSICAL POWER SYSTEMS

Power systems run in a balanced steady state three-phase configuration. Unfavorable and unavoidable events have the potential to disturb this state momentarily. Faults, also referred to as Short Circuits (SCs), is one of these abnormal events at which high levels of abnormal currents, of multiple magnitudes of the normal current, would flow in the system based on the location and the nature of the fault [71]. The

magnitude of these fault currents is influenced by both the impedance of the faulty circuit and the internal impedance of the generators that contribute to the faults. In classical power systems, large SGs are the main contributors besides a smaller contribution from some motors. SC faults are classified into balanced and unbalanced faults. They may occur at one or more phases in three-phase systems. As a result, they are categorized as single, double, and three-phase faults. Unbalanced faults encompass single line-to-ground, line-to-line, and double line-to-ground faults. While positive sequence components suffice for analyzing balanced faults, unbalanced faults require consideration of negative and zero sequence components. Faults are caused by the failure of the insulations in the system due to overvoltage which may occur because of lightning, switching surges, insulation pollution, conductor breaks from wind and ice loads, wind damage, trees cutting through power lines, shorting power lines by birds or small animals, etc. Fault analysis and the knowledge of the values and characteristics of fault currents is an essential task for several reasons. For instance, fault analysis in electrical power systems is necessary for health and safety considerations, design, operation, and protection of power systems [72]. Fault Level, also known as Short Circuit Capacity (SCC), is a critical parameter related to the maximum fault current. It is defined as the MVA associated with the maximum RMS symmetrical fault current, which typically occurs in the case of three-phase bolted faults as expressed in (1).

$$\text{Fault Level (MVA)} = \sqrt{3}V_L I_{SC} \quad (1)$$

where,  $I_{SC}$ , is the RMS fault current infeed, and  $V_L$  is the pre-fault voltage (line-line) at the faulty point.

The fault level MVA is a useful quantity for exemplifying the fault infeed from one or a group of SC contributing sources or an entire system at the faulty point. This might be more representative of the apparent power available during the faults which is utilized for several applications. By utilizing the fault level MVA, one can ascertain the suitable size of a busbar and assess the power system's strength or vulnerability, along with the equivalent impedance at the busbar [73]. It is also an alternative indicator for the fault contribution and the proper sizing of the system components such as the interrupting capacity of a circuit breaker. Moreover, it has been suggested as a valuable tool for conducting wide-area voltage stability assessments [74], estimating HVDC control applications [75], and evaluating the strength of multi-infeed LCC-HVDC systems [76].

Conventional power systems have historically been designed with a focus on high fault levels. This approach takes into account the substantial and time-decaying attributes of the fault current contribution from the synchronous generators (SGs), as illustrated in Fig. 5. SGs dynamic behavior during the period of the faults is inherent, and the time-decaying behavior is a result of the internal reactance of the SG, which exhibits a time-varying characteristics starting from the occurrence of the fault until the end of the fault duration.

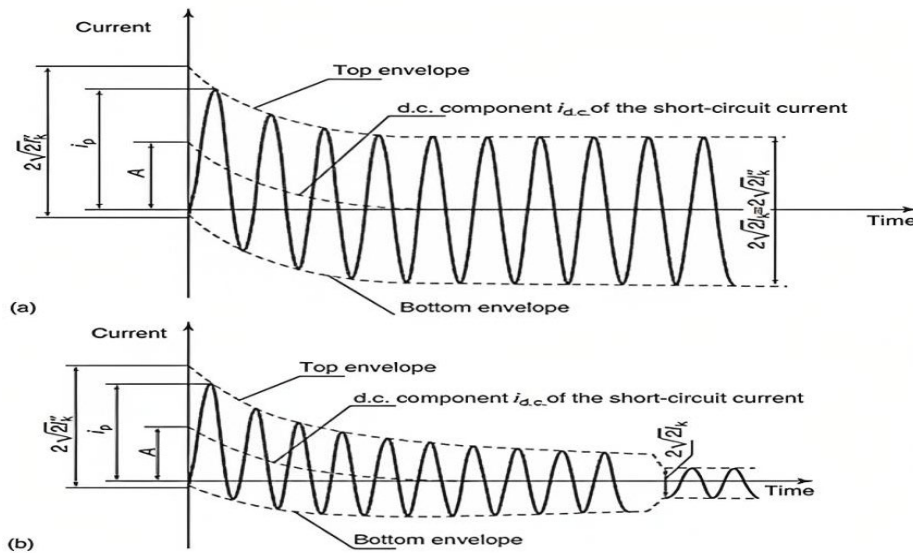


**FIGURE 5.** The fault currents contribution of the SGs a) far from generator, b) close from generator [77].

Hence, the SG is usually modelled using a voltage behind a variable reactance of three distinct variable values namely, the sub-transient reactance,  $X''$ , for the first few cycles of the fault, the transient reactance,  $X'$ , for around 5 cycles, and the synchronous reactance,  $X$ , for the rest of the period of the fault [77].

When addressing power system faults, both the impedance of the faulty path and the X/R ratio, extending from the generator terminal to the faulty location, significantly influence the resulting waveform during the fault. Apart from the symmetrical RMS value, a DC component may also emerge based on the timing of the fault initiation. In essence, the relative location of the faulty point in relation to the generator (proximity or distance) plays a crucial role in shaping the time-decaying behavior of the fault. Fig. 5 also shows the typical waveform of the faults in SGs-based power systems. Observe the initial symmetrical SC current ( $I_k''$ ), the peak SC current ( $i_p$ ), and the decaying DC aperiodic component ( $I_{dc}$ ) for faults occurring both close and far from the generator.

#### IV. GRID CODES AND FAULT-RIDE THROUGH REQUIREMENT OF PV AND WIND SOURCES

Grid Codes outline the technical specifications [78] needed to connect new generating units to the grid. Transmission System Operators (TSOs) work to set these criteria regularly throughout the world to guarantee the generation units' reliable and stable performance regardless of the grid's operation conditions [24], [46]. One essential aspect of grid codes, which provides guidelines for connecting RESs to the grid, is the Fault Ride-Through (FRT) capabilities, also referred to as Low Voltage Ride-Through (LVRT) [24], [27], [46], [48], [79], [80]. It specifies the needed functionality of the associated RESs (e.g., wind and PV) under abnormal circumstances, such as faulty conditions. RESs have historically

made a small contribution to system fault currents. Initially, neither power system operators nor grid codes issuers have considered the influence of RES on grid faults, leading to an absence of clear FRT requirements for these sources. Nevertheless, in response to the rising integration of RESs, modern grid codes now mandate RESs to ride through faults and supply dynamic reactive current injection to the grid [81]. The primary objectives of these requirements are to ensure uninterrupted power supply and avert any possible generation losses during and after significant grid failures [42], [43]. Various countries impose different FRT requirements for RESs based on several factors, such as the extent of RES penetration, the capacity of the generating unit, and the stability of the grid [48], [80].

##### A. THE VOLTAGE-VERSUS-TIME PROFILE

In Europe, each TSO is asked to submit a profile outlining the FRT specifications (voltage-versus-time (for transmission level's connected RESs. This requirement is set by ENTSO-E (the Transmission System Operators for Electricity) [82]. The general guidelines for the required profile are shown in Fig. 6. The diagram shows the minimum voltage that occurs at the connection point, expressed as a ratio of the actual voltage to the expected voltage, during normal operation and after a fault has occurred. where  $U_{ret}$  is the connection point's retained voltage.  $T_{clear}$  indicates when a fault has been cleared. In addition, certain points of the lower limits of voltage recovery after fault clearance are specified by  $U_{rec1}$ ,  $U_{rec2}$ ,  $t_{rec1}$ ,  $t_{rec2}$ , and  $t_{rec3}$ . Table 1 presents guidelines and recommendations for these parameters' values.

It should be noted that unless the internal electrical faults protection scheme necessitates the disconnection of the power generating module from the network, the RESs must remain connected and maintain a stable response during fault

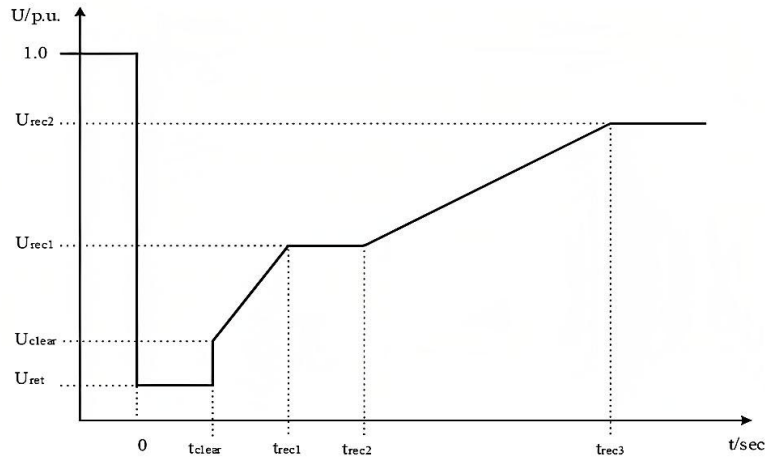


FIGURE 6. The voltage-versus-time FRT profile according to ENTSO-E [82].

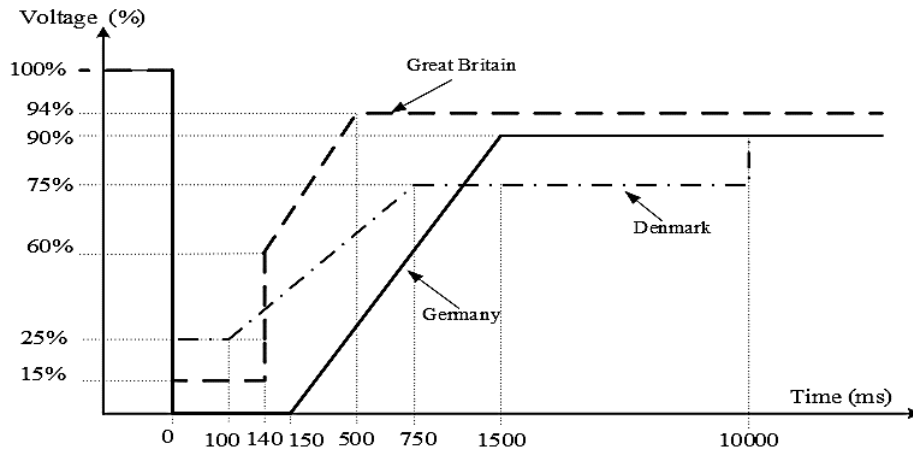


FIGURE 7. The national voltage-versus-time FRT profile for selected grid codes in Europe [47].

occurrences. Additionally, it is important to highlight that FRT capabilities are usually specified by each TSO in the case of asymmetrical faults [82].

Customized FRT capability profiles have been defined by some of the individual national grids, as shown in Fig. 7 for some of European countries such as Great Britain, Denmark, Italy, and Germany [47], [83]. It is noteworthy that certain grid codes in countries such as Sweden, Finland, Germany, and Spain mandate RESs to possess zero voltage-ride-through capability [28].

**B. REACTIVE-CURRENT INJECTION**

Besides the voltage-versus-time profile requirement that set the period where the generator shall remain connected, RESs are obligated to offer dynamic reactive voltage support during faults. Hence, generators must be capable of supplying reactive current in accordance with their current rating for a specific duration, while also reducing active power output if required during the fault [25], [29], [44], [84]. This is

TABLE 1. FRT parameters of the voltage-time-profile in Fig. 6 [82].

	Voltage Parameters (p.u.)		Time Parameters(s)	
$U_{ret}$	0.05-0.15	$t_{clear}$	0.14-0.25	
$U_{clear}$	$U_{ret}-0.15$	$t_{rec1}$	$t_{clear}$	
$U_{ret1}$	$U_{clear}$	$t_{rec2}$	$t_{rec1}$	
$U_{ret2}$	0.85	$t_{rec3}$	1.5-3.0	

common in large interconnected systems because it is more important to contain the voltage dip within a specific area by supporting the voltage rather than worrying about the potential consequences of reducing active power. Although it might be more important to maintain active power output in islanded systems because its reduction can have severe consequences

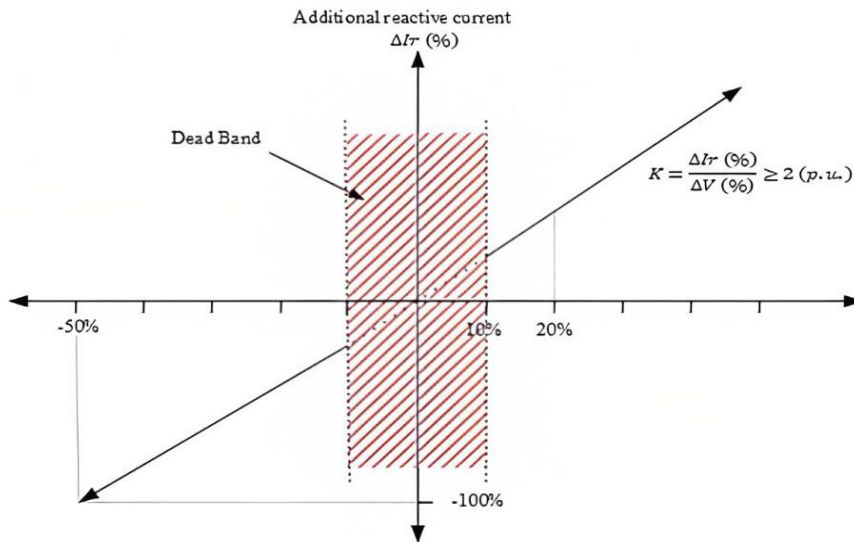


FIGURE 8. The requirement for reactive current injection as per German grid code [26].

for system frequency, in some cases, the grid may still require a dynamic requirement for reactive current [25]. Through the injection of additional reactive current, the voltage dip during a fault is bolstered, facilitating voltage recovery after the fault. As a result, the necessary fault current for protective systems is supplied [44].

Remarkably, most grid codes typically require a positive sequence current injection (balanced currents) even during unbalanced faults [29], [50], [84]. Nevertheless, recent research has started to consider unbalanced currents during such faults. The quantity of reactive current injected by the FRT control system varies depending on the specific grid code in effect. For instance, grid codes in Great Britain and Denmark mandate generators to inject the maximum attainable reactive current during a fault [85].

Conversely, the German grid code necessitates a proportional gain approach [23], [86]. The proportional gain, often known as the k-factor, establishes the proportion of the reactive current that should be injected during a fault based on the voltage dip observed at the terminal of the RES-based generator. Consequently, the fault current level is determined by the voltage level. According to the German grid code, this gain can typically vary from 2 to 10, as illustrated in Fig. 8 [26], [86]. It is important to recognize that maximizing the k-factor would subsequently decrease the value of the injected active current accordingly. However, the maximum fault current of the RES would be restricted by the maximum overrating capability of such resources.

Note that most grid codes require RESs to only inject positive sequence current components even in response to unbalanced faults [87]. However, providing positive sequence reactive current only from RESs in asymmetrical faults may lead to increasing the voltage level in all healthy and faulty phases [88], [89]. So, recent grid code updated the reactive

current injection and voltage support requirement to account for this issue. For instance, recent grid codes defined by Spanish, German, and Greek TSOs account for the negative sequence injections during asymmetrical faults [90].

## V. FAULT CURRENT CONTRIBUTION OF PV AND WIND SOURCES

The fault current contribution of a PV or wind energy source refers to the amount of electrical current that the source can provide in a power system during a fault or SC condition. In PV systems, this contribution is predominantly influenced by the utilization of a converter-interface for grid integration. Through the grid-side connected converter, PV systems regulate their fault current contribution. However, it is noteworthy that not all wind generators are equipped with such converter-interfaces, leading to variations in fault current behavior among wind energy sources [91], which lead to a variety of SC current characteristics and fault current contributions according to the technology used for grid interface purpose. This section aims to provide a detailed insight into the up-to-date reports and studies in the literature concerning the fault current contribution from PV and different wind technologies. It is worth noting that utility-scale wind power plants can be classified into five categories based on their machine type, ability to control speed, and other operational characteristics, according to IEC 61400-27 [92]. These are squirrel-cage induction generator (Type-I), wound rotor induction generator with external rotor resistance (Type-II), doubly-fed asynchronous generator (Type-III), full power converter generator (Type-IV), and SG mechanically connected through a torque converter (Type-V) [92]. However, from the converter-interface point of view, these in addition to the PV systems (which are connected through converter-interface to the grid), can be recategorized in a

different way. Therefore, to distinguish between the different fault current contributions according to the technology and the grid interface method, these RESs are categorized into four categories: Those RESs i) directly connected sources without converter interfaces, ii) those partially converter-interfaced sources, iii) fully converter-interfaced sources, and iv) mechanical torque converter-interfaced Sources.

These categorizations are devised to account for the presence of converter-interfaces, aiming to refine the characterization of fault behavior in both PV and wind energy systems. It is essential to note that the grid-side converter interface, when available, assumes primary control over fault current contribution, regardless of the generator-side technology utilized. Consequently, the subsequent sub-sections are structured according to how the generation source interfaces with the grid: either directly without a converter, partially with a converter, or fully through a converter grid interface.

**A. DIRECTLY CONNECTED SOURCES WITHOUT CONVERTER-INTERFACE**

**1) TYPE-I WIND**

The utilization of induction generators in the majority of commercial wind turbine installations worldwide stands out as a notable characteristic of wind turbine generators linked to the AC network. This predominance of induction generators, in contrast to SGs, constitutes a significant differentiation, given that nearly all directly-connected commercial wind turbine installations worldwide opt for induction generators [72], [92]. Initial utility-scale wind turbine generators typically feature fixed-rotation-speed turbines paired with squirrel-cage induction generators (SCIGs). These generators operate at speeds slightly higher than synchronous speed, with the difference termed as slip, often measured in percentage. Negative slip denotes electricity generation. Standard operating slips for induction generators usually range from 0% to -1%, with modern large turbines commonly operating at -1%. Essentially, these generators rely on wind turbine prime movers operating just above synchronous speed, employing blade pitch angle control for primary wind power regulation. According to most of studies in the literature, SCIG wind generators offer mechanical simplicity, high efficiency, and minimal maintenance needs as key advantages [93], [94]. They are known as Type-I wind generators. In other studies, they are frequently labeled as “fixed-speed” turbines owing to their minimal speed variation from no load to full load [33]. It is worth noting that the pitch angle controller, the turbine, the driving shaft employing a two-mass model, and the SCIG are the essential building pieces of the wind turbine dynamic model [31]. As slip fluctuates, corresponding variations occur in the real power output within the rated slip range. Induction generators inherently consume reactive power during both generation and operation. With increasing output power, reactive power demand rises significantly. Fig. 9 illustrates a Type-I wind generator grid-connected via a pad-mounted transformer with switched

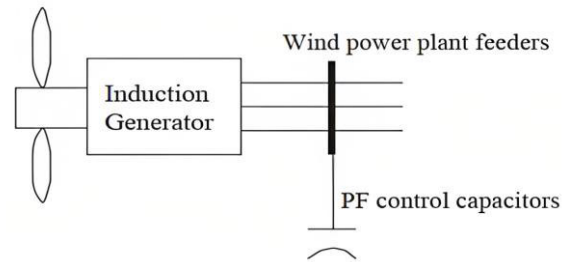
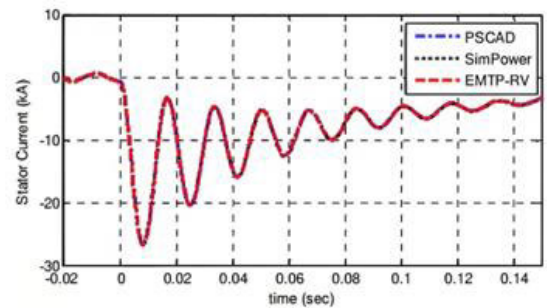
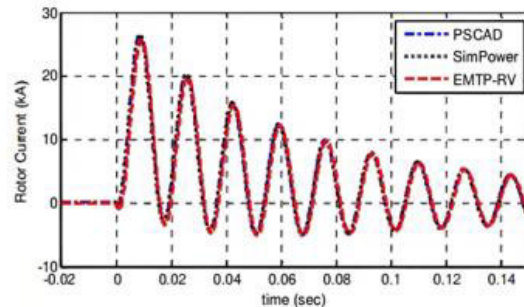


**FIGURE 9. A grid-connected Type-I wind generator [92].**



**(a)**



**(b)**

**FIGURE 10. Phase A current of type-I wind generator during three-phase SC: a) stator, b) rotor [95].**

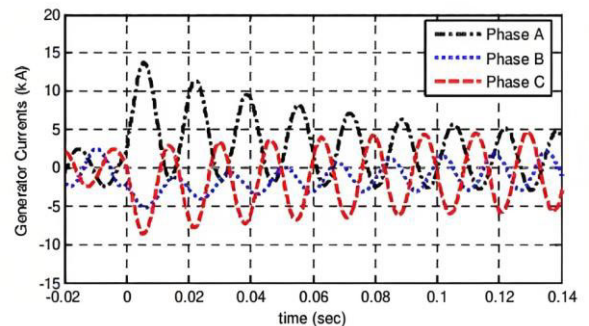


**FIGURE 11. Three-phase currents of type-I wind generator during single-phase-to-ground SC [95].**

capacitor banks to maintain the induction generator at unity power factor [92].

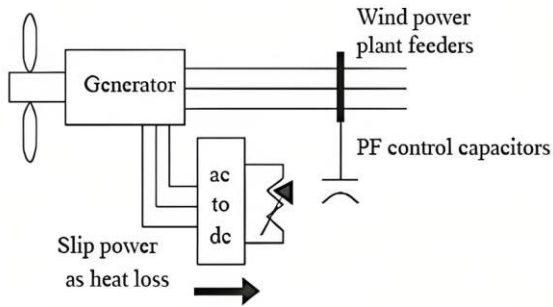


FIGURE 12. A grid-connected Type-II wind [92].

Type-I wind generators have a high potential for generating fault current, with their initial contribution during a fault potentially may go up to six times of their rated current or more, depending on the timing of the short circuit. However, this magnitude decreases as the fault continues [31], [33]. For SC calculations, this type of generator is modelled therefore by a voltage behind an inductance that represents the sub-transient initial asymmetrical contribution accordingly. In [95], the voltage behind the inductance model has been suggested to calculate both symmetrical and asymmetrical fault current contributions by solving for the fault current at the inception instant of the fault using sequence component networks.

It is important to consider that various factors can influence the fault current contribution of wind turbine generators, such as magnetic saturation, deep bar effects, and the stator's winding connection. Therefore, models should offer options for simulating saturation and representing the deep-bar characteristics of large induction machines, often accomplished through the use of a double-cage rotor [95]. In accordance with [96], the transient reactance dominates the induction generator fault current opposing the SG, where the machine's sub-transient reactance dominates the fault current. Compared to a SG, the fault current contribution of an induction generator lasts significantly longer. During three-phase-to-ground faults, the type-I wind generator exhibits a high initial fault current, which rapidly reaches high SC currents immediately after the fault inception. However, this contribution gradually decays to zero over time during the fault duration, likely due to the loss of an external source of excitation, as shown in Fig. 10. On the other hand, phase-to-ground faults may result in fault currents with lower levels compared to three-phase faults, as expected. Nonetheless, the other healthy phases continue to provide excitation and maintain the connection to the grid, resulting in fault currents that do not decay to zero [96]. Refer to Fig. 11 for an illustration of the current waveform of the three-phase currents of the type-I wind generator in response to a single-line-to-ground fault at phase A.

## 2) TYPE-II WIND

Wound rotor induction generators with external rotor resistance are referred to as Type-I wind generators. Type-II

wind generator is a variable-slip wind turbine with a wound rotor where a three-phase external resistance is connected to the rotor through a PE component (i.e., converter) [93]. As indicated in [72] and [94], employing a converter-external resistance setup enables the adjustment of rotor circuit resistance to tailor torque-speed characteristics. Essentially, this technique facilitates control over rotor current and electromagnetic torque levels, allowing the generator's speed to vary within a limited range, typically up to 10%. Compared to the Type-I wind generator configuration; this affords a broader spectrum of operating speeds. Nonetheless, implementing the converter-external resistance arrangement entails additional costs and increased losses, which are dissipated through the external resistance. Similar to Type-I generators, Type-II wind generators utilize a capacitor bank to provide the necessary reactive power when connected to the grid, as depicted in Fig. 12. During low to medium wind speeds, a Type-II wind generator functions similarly to a Type-I generator, with no external resistance introduced. Consequently, the external resistance is short-circuited, exerting no influence on generator operation. However, in high wind speed conditions nearing the rated slip, the external resistance is engaged, resulting in operational disparities between Type-I and Type-II generators. The SC characteristics of type-II wind generators might be to an extend like type-I if the effect of the external resistance is ignored. However, it is reported in [32], the introduction of external resistance leads to a more damped fault current.

Consequently, the fault current contribution in Type-II generators is lower compared to Type-I due to the damping effect of the external resistance. Therefore, neglecting the impact of external resistance on Type-II dynamic behavior could potentially lead to misleading conclusions. As per the most of relevant literature, the fault contribution of type-II wind generator in response to a three-phase faults, shows a high initial fault current that reaches high SC levels immediately after the instant of the fault. Like Similar to Type-I generators, the fault current contribution of Type-II generators gradually diminishes to zero over time during the fault period. This trend is evident in Fig. 13, depicting the response of a Type-II wind generator to a three-phase fault at the generator terminal. Additionally, Fig. 14 illustrates both the AC and DC components present in the fault current contribution of Type-II wind generators [32]. Observe the large DC offset that also decays with the time in addition to the instantaneous current component that never decays completely down to zero. While the external resistance might affect the damping of the fundamental component, it might not affect the rate of decay of the dc component [32].

In other study conducted in [94], the presence of external rotor resistance is noted to reduce the decay time of the current. Overall, the fault contribution and behavior of both Type-I and Type-II wind generators are comparable, exhibiting nearly identical responses. However, because of external rotor resistance which reduces the SC current, the fault contribution for type-II wind

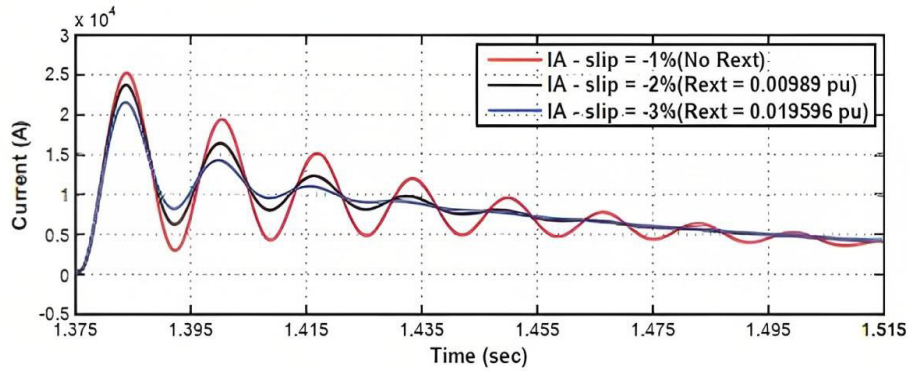


FIGURE 13. The response of type-II wind generator to a three phase SC with and without external resistance [32].

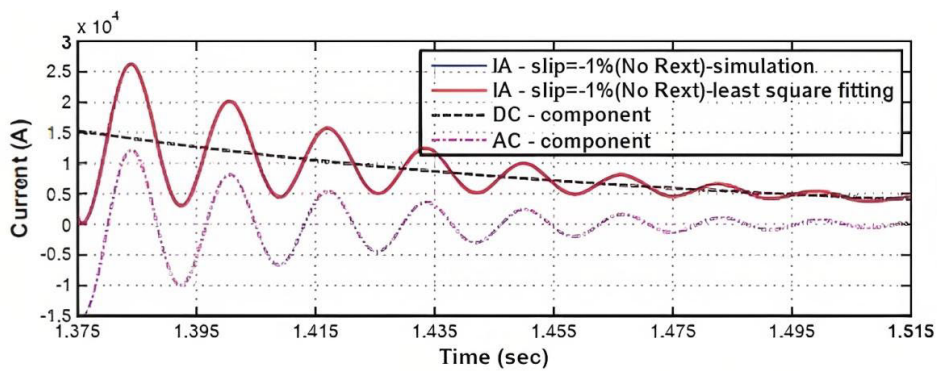


FIGURE 14. The AC and DC components of the current response of type-II wind to a three phase SC [32].

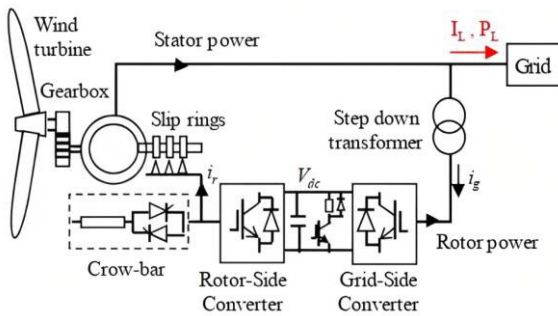


FIGURE 15. Typical layout of Type-III wind generator [36].

generator may be less than the fault current from a type-I.

**B. PARTIALLY CONVERTER-INTERFACED SOURCES (TYPE-III WIND)**

Wind turbines that utilize Double-Fed Induction Generators (DFIG) are referred to as type-III wind generator. In such generators, the stator is straight connected to the grid while the rotor, which employs a wound rotor induction generator, via a power electronics interface (i.e., converter). This is represented by a bi-directional back-to-back Voltage Source

Converter (VSC). Hence, the power exchange with the grid is partially done through converter-interface. Therefore, they are also referred to as partially-converter-interfaced wind generators. Among other types of wind generators, DFIG technology is considered the highest proportion of wind generator installations globally [97], [98], [99]. One of the main distinguished features of DFIG is that the partially-grid connection topology would enable the generator to operate at a variable speed of a typical range of  $\pm 30\%$  of the synchronous speed [97]. This allows voltage support capabilities and a decoupled control of active and reactive power. Moreover, Type-III wind generators have also lower power losses when compared to fixed-speed induction generators (Type-I) or SGs that utilize full converter-interfaced converters [100], [101]. Fig. 15 shows a typical layout of a Type-III wind generator where a step-up transformer is connecting the stator to the grid, and a back-back VSC is connecting the rotor windings via slip rings [72]. The task of the converter at the rotor side is to feed the rotor circuit a three-phase voltage at slip frequency. The converter controller can change the injected voltage's magnitude and phase in such a way as to regulate the rotor currents nearly instantly. Note that the VSC is designed with limited thermal and voltage capabilities, as it would partially exchange the power with the grid. However,

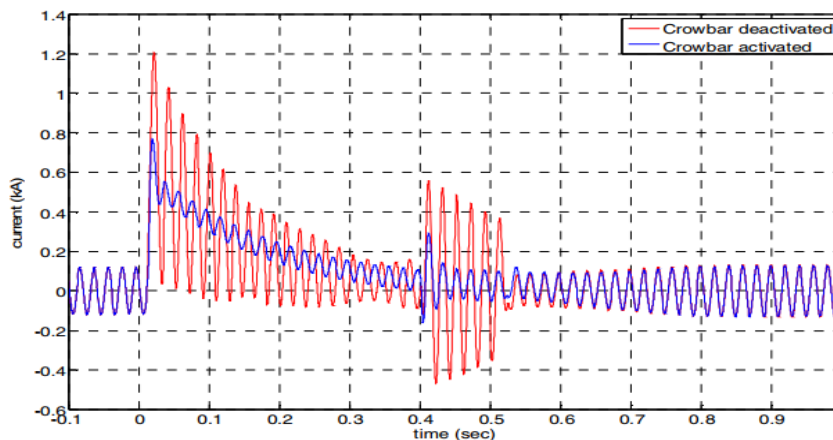


**FIGURE 16.** The effect of the crowbar resistance insertion on the SC current of type-III wind generator [104].

a proper protection arrangement accompanies the design in such a way to allow the generator to meet the requirements of grid codes and FRT. Such protection would protect the IGBTs switches employed in the converter from high DC voltages and high rotor currents by integrating a chopper circuit that is connected to the DC link [40]. To protect the rotor in case of excessive currents, a crowbar circuit is introduced in the rotor circuit. Although this crowbar circuit might provide proper protection for the rotor against high and excessive currents, it can lead to undesired loss of controllability of the machine side converter. This is because the insertion of such a crowbar circuit is usually accompanied by deactivation of that converter.

The crowbar protection system comprises a three-phase diode bridge rectifier, a bypass resistance, and a switch. In conventional crowbars, the switch is typically a thyristor, while active crowbars use semiconductor switches like isolated gate bipolar transistors [49]. In fact, the crowbar circuit significantly affects the fault response of Type-III wind generators [35], [49], [102]. In any faulty conditions, the converter switches are promptly shut off, and the thyristors of the crowbar circuit are activated to prevent a significant overvoltage on the DC link. The converter is short-circuited and bypassed by this crowbar action, allowing the rotor currents to enter the crowbar circuit to prevent the instantaneous rotor current from exceeding the permissible converter limit, hence protecting the converter [20], [22], [45].

According to the research implemented in [20], the activation of the crowbar circuit is influenced by the severity of the voltage dip that would result from the faults. For instance, the crowbar circuit might not be activated during shallow faults (e.g., faults far from the wind generator). In such cases, the generator may hold active and reactive power exchange as normal. Therefore, an ideal current source model for fault calculation might be utilized [103]. On the other hand, the crowbar circuit would be activated in case of a large voltage dip because of a severe fault. In such conditions, the crowbar effect would be significant, and it should be considered when

accounting for the fault current contribution from Type-III wind generator [104]. In that case, the ideal current source model for fault calculations would not be able to represent the fault contribution, and other models should be considered. Fig. 16 shows the reduced SC contribution by Type-III wind generator in case of activation of the crowbar circuit. Observe that the activation of the crowbar would approximately reduce the initial fault current contribution to 50% of the one that is observed without crowbar activation. Note that the crowbar resistance also affects both the time constant of the rotor and the maximum peak value of the SC current. Due to fast activation and deactivation of such a crowbar circuit, the DFIG shows non-linear behavior in the first few cycles affected by the discrete operation of the crowbar as shown in Fig. 17 [105]. During a severe balanced three-phase SC event, the DFIG exhibits a specific response. Initially, the rotor circuit is crow-bared in response to the SC occurring at the step-up transformer, causing a voltage drop down to (0.2 p.u.). This limitation results in the symmetrical current produced being restricted to approximately (4 p.u.). After the fault is cleared, the crowbar is deactivated, but it reactivates again if the fault level rises. Consequently, this sequence of events leads to highly discontinuous fault behavior of the DFIG [105]. It is worth noting that the initial RMS SC current contribution for wind generators, specifically Type-I and Type-III, can reach up to (5 p.u.), with the maximum instantaneous peak value falling within the range of (6 to 10 p.u.) during the first cycle. Additional research in [106] has suggested that the fault current of Type-III wind generators might also reach values between (5 to 6 p.u.) for faults directly applied to the generator's terminal [36], the DC chopper circuit that might play the main role in protecting the DFIG generator in response to a high voltage level at the DC link. This in turn would block the crowbar, which would act as a backup protection that works only if the DC chopper fails to operate properly. Hence, it is important to distinguish between the SC current contribution in both cases [36]. Moreover, it is worth noting that modeling the fault contribution of the DFIG when

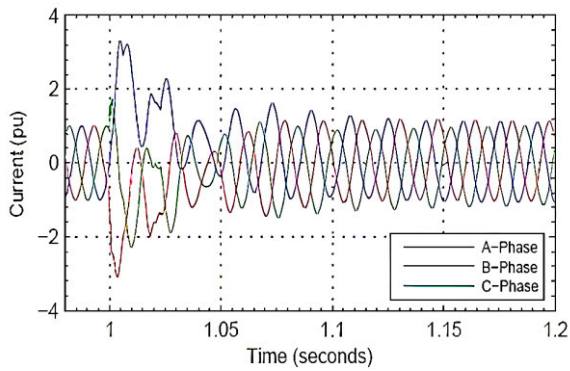


**FIGURE 17.** Impact of the discrete operation of the crowbar on SC current of type-III wind generator [105].

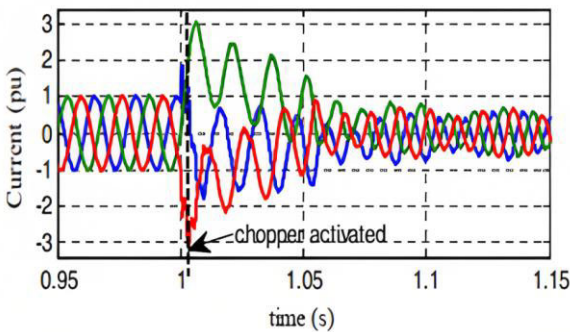


**FIGURE 18.** Type III wind farm output currents with DC chopper activated and deactivated crowbar [105].

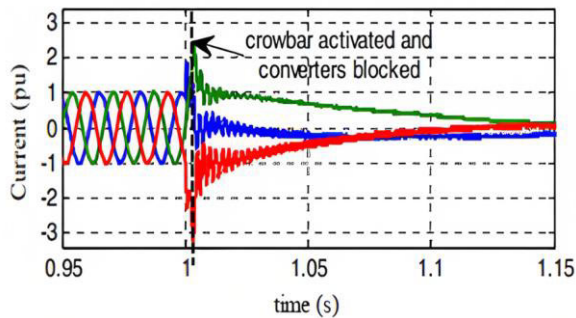


**FIGURE 19.** Type III wind farm output currents with DC chopper deactivated and activated crowbar [105].

crow-bar is considered, seems complex and the response cannot be captured by a single equivalent model. Although, some models like an equivalent voltage source-impedance series is proposed for calculating Type-III DFIG's peak current according to IEC 60909 [103], their extensive reliance on proprietary control schemes and transitions between normal and crowbarred states making a generic fault model imprecise across a range of fault severities.

Fig. 18 shows type III wind farm output currents with DC chopper activated and deactivated crowbar. Observe the fault current contribution with a high DC component due to the sudden voltage change at the instant of the fault. Regardless of the activation of the DC chopper circuit, it can be observed

that a high fault current is still seen with a high DC component that it decays over the time.

The maximum instantaneous fault current might reach high value up to 3 p.u., as shown in Fig. 18. On the other hand, in the case at which the DC copper circuit is deactivated but the crowbar is activated, a lower level of fault current is resulted with a limited maximum instantaneous value to around 2 p.u. Also, Fig. 19 shows that the DC component is suppressed compared to the situation when DC chopper activated and deactivated crowbar (Fig. 18) [36].

Note that in the second case in which the activation of the crowbar takes place, the converter would be blocked and the fault response of the DFIG would be almost identical with what has been observed from Type-I (i.e., fixed speed squirrel cage induction generator). Regardless of the control objectives, Type-III wind generators may show a limited and predictable steady-state fault contribution, as discussed in [107].

In summary, the behavior of the DFIG is influenced by the fault severity, the applied protection scheme, and the activation of either the DC chopper circuit or the crowbar circuit. These factors collectively dictate the response of the DFIG during fault conditions. Note that Table 2, summarizes SC characteristics, modeling approaches, and the influencing factors of directly connected or partially converter-interfaced sources (Types I, II, and III).

### C. FULLY CONVERTER-INTERFACED SOURCES

Unlike the previously discussed sources, fully converter-interfaced sources employ full size converters in their interface for grid connection purposes. Hence, their fault current contribution is mainly controlled and governed by the grid side converter, its capability and control algorithms. These sources include type-IV wind generators and PV systems. This section provides a detailed insight on these technologies, an up-to-date literature on the SC characteristics, and the fault current contributions in response to SC faults in the system.

#### 1) TYPE-IV WIND

Utilizing full interfaced-converter to connect the electrical generation units in Type-IV wind, means to completely isolate the generator from the system by this converter. In such case, the SC current produced is determined by the grid side converter [18], [34]. Figure 20 depicts the typical full interfaced-converter used for integrating Type-IV wind generators into the electrical power system. These wind turbines utilize an electrical generator, which can either be an asynchronous machine (induction generator) or a SG excited by either electricity or permanent magnets. If an asynchronous generator is used, a gearbox is often incorporated into the design. The Type-IV wind turbine design, employing a full-rated converter interface, offers exceptional flexibility in power generation by enabling the generator to rotate at the optimal aerodynamic speed. As a result, the electrical output is entirely controlled by the converter interface rather

**TABLE 2. Summarized fault characteristics, modeling, and influencing factors of types I,II, and III wind sources.**

Attribute	Type-I (Squirrel-Cage Induction Generator)	Type-II (Wound-Rotor Induction Generator)	Type-III (Doubly-Fed Induction Generator)
<b>Grid Interface</b>	<ul style="list-style-type: none"> <li>- Directly connected to the grid without power electronic converters</li> </ul>	<ul style="list-style-type: none"> <li>- Directly connected to the grid with external rotor resistance control</li> </ul>	<ul style="list-style-type: none"> <li>- Stator connected to the grid via transformer;</li> <li>- rotor connected through partially-rated back-to-back VSC via slip rings</li> </ul>
<b>Fault Modeling Approach</b>	<ul style="list-style-type: none"> <li>- Thevenin-equivalent voltage source behind transient reactance, including sub-transient behavior and DC offset (IEC 60909-based)</li> </ul>	<ul style="list-style-type: none"> <li>- Similar to Type-I Thevenin model with added external rotor resistance for damping and decay</li> </ul>	<ul style="list-style-type: none"> <li>- Ideal controlled current source during normal converter operation and shallow faults.</li> <li>- voltage source-impedance model when the converter is blocked and crowbar is activated.</li> <li>- IEC 60909-based equivalent voltage source-impedance model for peak current estimation.</li> <li>- Hybrid modeling required</li> </ul>
<b>Fault Current Contribution</b>	<ul style="list-style-type: none"> <li>- Initial RMS up to 5 p.u.</li> <li>- Peak current: 6–10 p.u.</li> <li>- AC and DC components</li> <li>- Rapid decay</li> </ul>	<ul style="list-style-type: none"> <li>- Reduced peak and RMS currents</li> <li>- AC and DC components</li> <li>- Faster decay</li> <li>- Damped response</li> </ul>	<ul style="list-style-type: none"> <li>- Initial RMS: 5–6 p.u.</li> <li>- Peak current: 6–10 p.u.</li> <li>- Discontinuous behavior</li> <li>- Reduced current under crowbar</li> </ul>
<b>Influencing Factors</b>	<ul style="list-style-type: none"> <li>- Magnetic saturation</li> <li>- Rotor characteristics</li> <li>- Stator configuration</li> <li>- Operating slip</li> <li>- Grid strength</li> </ul>	<ul style="list-style-type: none"> <li>- Rotor resistance control</li> <li>- Wind speed</li> <li>- Fault timing</li> <li>- Grid impedance</li> </ul>	<ul style="list-style-type: none"> <li>- Fault severity</li> <li>- Crowbar parameters</li> <li>- Protection timing</li> <li>- Converter limits</li> <li>- FRT control strategy</li> </ul>
<b>Remarks</b>	<ul style="list-style-type: none"> <li>- Current decays after faults</li> <li>- Sustained current in single-phase faults</li> <li>- Longer contribution than SGs</li> <li>- Depends on pre-fault conditions</li> </ul>	<ul style="list-style-type: none"> <li>- Type-I-like behavior at low wind speeds</li> <li>- External resistance bypass in normal operation</li> <li>- Improved controllability</li> <li>- Capacitor-based reactive support</li> </ul>	<ul style="list-style-type: none"> <li>- Strong dependence on protection scheme</li> <li>- Limited steady-state contribution</li> <li>- No universal equivalent model</li> <li>- IEC 60909 mainly suitable for peak current</li> </ul>

than being solely determined by the inherent behavior of the generator [106]. Fig. 20 also illustrates the components of the fully converter-interfaced (Type-IV wind) that includes; AC to DC converter (generator side), DC link, and DC to AC inverter (grid side). The DC link allows the inverter to be regulated and deliver output power regardless of the input power, as long as it remains within the manufacturer-specified voltage range. Additionally, the inverter is adjusted to coincide with the collector system's frequency (to remain synchronized). However, manufacturers' inverter control strategies can differ significantly. To increase the voltage from a range of (400-690 V) up to the collector system voltage level, which is normally 34.5 kV in North America and 33 kV in Europe, a transformer unit is attached to the inverter's output [108]. Based on the above discussion on the configuration of Type-IV wind generator, it would be observed that the SC current contribution is fully controlled and governed by the grid side converter-interface. More specifically, the SC signature of Type-IV wind generators is mainly dictated by the control strategy implemented in the converter interface, which can vary significantly between manufacturers. In general, most Type-IV wind generators inject only a symmetrical fault current contribution, regardless of whether the fault is balanced or unbalanced [87].

Hence, neither the negative nor the zero components are considered like the case of SGs which are providing such

components during unbalanced faults. Typically, the fault response of Type-IV wind generators is usually depicted as a rapid transient followed by a steady-state current in the fault contribution, as illustrated in Fig. 21. An initial overshoot occurs right after the fault initiation, lasting for a brief period (one or two cycles), with the current potentially reaching up to (3 p.u.), subject to the manufacturer's design and characteristics. According to [39], the transient current includes high-frequency components and can persist for a duration of two cycles. As explained in [15], the magnitude of this transient is influenced by various factors, including the pre-fault operating conditions, the voltage dip experienced during the fault, and the rate of reactive current injection. On the other hand, once this transient is completely decayed, the fault current is controlled to a limited value which might vary according to the overrating capability, the fault severity, and the LVRT gain ( $k$ -factor explained earlier in Section IV). The steady-state maximum controlled current is restricted to a range of (1.1-1.6 p.u.) of the rated current of the converter interface [105]. According to [33], for most inverters of this type, the maximum current is limited to (1.1 p.u.), implying that Type-IV wind generators are designed with an overloading capability of only 10% above their rated current.

Recently, in response to the updated grid codes as discussed earlier in Section IV, manufacturers started to pay attention to the importance of the capability of the

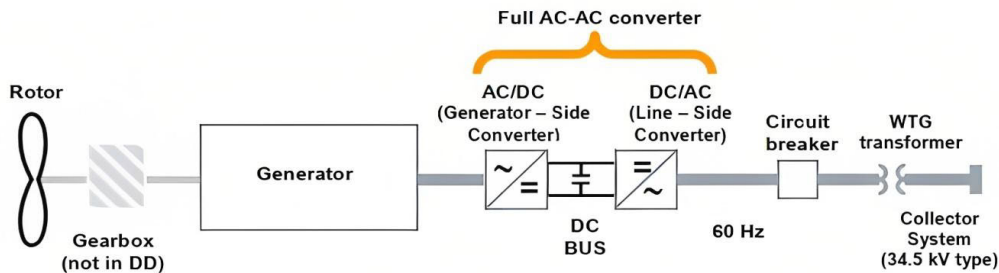


FIGURE 20. Typical layout of Type-IV wind generator [34].

converter to provide negative sequence component injections with Type-IV wind generators in response to unbalanced faults [90]. As reported in [109], the VSCs used in wind generators respond to unbalanced faults as controlled current sources in both the positive and negative sequence circuits. However, the zero sequence does not contribute significantly to faults due to transformer configuration, which leaves the zero-sequence circuit open-circuited in most applications. Nevertheless, the inclusion of negative and zero sequence components might lead to considerable ripple on the DC bus, potentially requiring a larger capacitor [88]. Consequently, some manufacturers prefer to inject positive sequence fault current only, even in the case of unbalanced faults. This results in a simplified and nearly uniform fault response of Type-IV wind generators regardless of the fault type. Fig. 22 illustrates the comparison of fault current contributions of Type-IV wind generators in response to balanced and unbalanced faults. Note the marginal difference, which may be confined to a lower transient in the case of a single-line fault (Fig. 22, b) compared to a balanced three-phase fault (Fig. 22, a).

During unbalanced faults, another notable distinction is the lower current components observed in the healthy phases (B and C). These healthy phases do not reach the maximum limit, unlike the faulty phase (A) which does. Importantly, the fault current remains within the converter's upper limit of (1 p.u.).

## 2) PV SYSTEMS

Solar energy is captured and converted into electricity by PV systems to produce power. The generated power is in the form of DC voltage and current, so electricity must be converted using power electronics converters before it can be used locally or fed into the electrical grid. Therefore, like Type-IV wind generators, the converter interface design and control determine how much of a fault contribution comes from the PV systems. Fig. 23 shows the configuration of a PV system which is connected to the grid through a converter interface arrangement [110]. It can be observed that the PV panel is initially linked to a DC/DC boost converter (DC chopper) before being incorporated into the AC grid via the DC/AC converter interface. The converter interface serves to

insulate the PV system from grid malfunctions. Therefore, examining the converter interface's performance during faults becomes essential in comprehending the PV system's fault response.

Note the controlled SC response of the inverter during the fault along with the activated current limiter and the DC chopper circuit would determine such performance of the PV system during the faults. In other words, the power electronics employed in the converter interface and the algorithms utilized in the controllers allow for some degree of control over how PV systems respond to short circuits [111].

Like the SC response of Type-IV wind, PV system may contribute to a limited positive sequence fault current when equipped with a FRT capability to remain connected and to inject reactive current during a SC fault [112]. However, it can be observed from Fig. 24, that the transient is very fast and limited to around 200% of the converter's rated current the manufacturer allowed for inverter oversizing otherwise it is mainly limited to around (1p.u. to 1.2p.u.) [111]. Another piece of experimental research has shown that some converters may contribute to a very high transient (up to 600% of the rated current), but it lasts for very limited time of 1 millisecond [19]. It is worth noticing that the time at which the transient may last is dependent also on fast fault injection as well as the speed of fault detection and activation of the FRT control [15].

Conversely, when considering the steady-state fault current contribution, it becomes evident that the currents in all faulty phases are restricted to approximately the rated currents. In simpler terms, the currents before and after the fault exhibit striking similarities. However, this steady-state fault current contribution might show higher or lower levels in some other case depending on the overrating capability and the current limits defined in the controller. When faced with unbalanced faults like single line to ground and double line faults, the PV system might not exhibit a substantial disparity in the fault current contribution. Nevertheless, the current level supplied during the fault could be influenced by the pre-fault operating conditions.

In [19] and [30], the SC response of a PV to both single and double line to ground SC faults were studied and it was

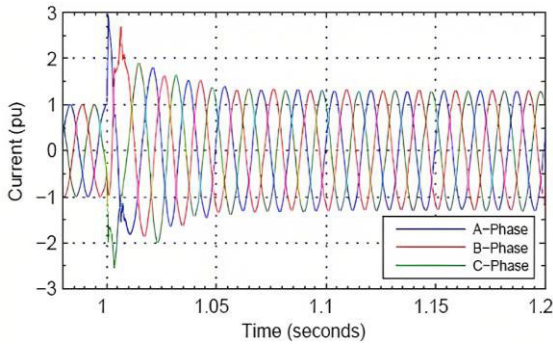


FIGURE 21. SC current contribution of a Type-IV wind generation unit [105].

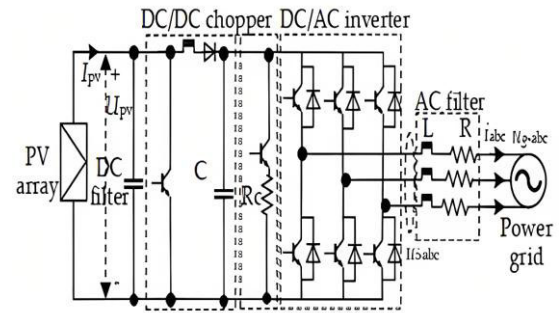
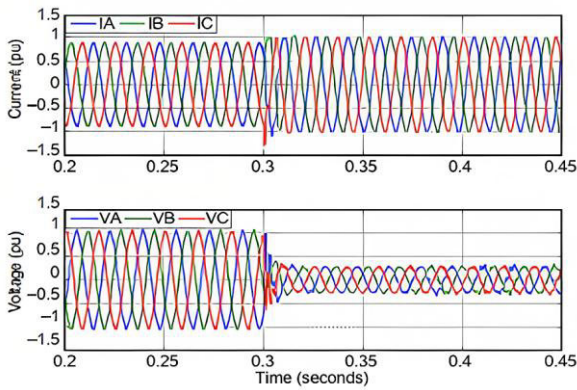
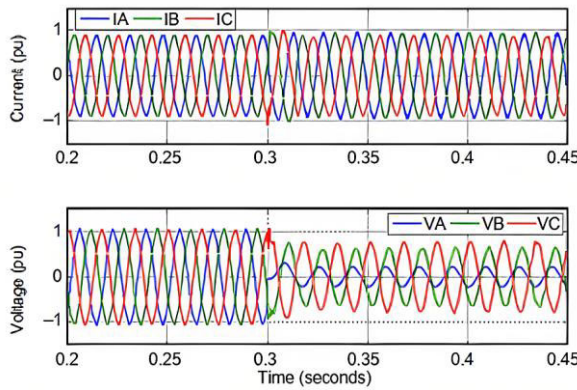


FIGURE 23. Layout of grid-connected PV system [110].



(a)



(b)

FIGURE 22. SC current contribution of a Type-IV wind generation unit in case of, a) three-phase balanced fault, b) single-line fault at phase A [90].

concluded that the response of PV system under both faulty conditions are almost the same. However, the later fault (i.e., double-line to ground fault) may experience a higher current contribution, as shown on Fig. 25. It can be observed that a very fast transient (almost negligible) has appeared at the instant of the single-line to ground fault that is accompanied by a steady-state fault current. However, at the instant of the double-line to ground fault at 9.09 s, the PV system has responded with a higher value of a steady-state SC current of approximately 0.7 p.u.

#### D. MECHANICAL TORQUE CONVERTER-INTERFACED SOURCES (TYPE-V WIND)

In type-V turbines, a synchronous generator (SG) and a torque/speed converter are integrated into a conventional wind turbine generator's variable-speed drive train [106]. The torque/speed converter assumes a pivotal role in controlling the output speed by transforming the variable speed of the rotor shaft into a consistent output shaft speed. Utilizing a wound rotor type SG, the variable speed wind generator implements this design, facilitated by the mechanical converter's regulation of speed and torque. This approach represents a conventional concept in variable speed operations, as reported in [41]. The speed/torque converter, also referred to as a variable ratio transmission, serves the function of converting variable speed into fixed speed. Fig. 26 illustrates the typical configuration of a Type-V wind generator. In this setup, the SG operates at a constant speed aligned with the grid frequency and is directly connected to the grid via a synchronizing breaker. Apart from regulating the speed and torque of the converter, alongside the conventional Automatic Voltage Regulator (AVR), the grid-connected SG necessitates inclusion of a synchronizing system and protection system. The fault response of the Type-V wind generator mirrors the standard behavior of a SG [106]. The level and characteristics of the SC current of SGs are well-known and understood [38], [73], [113], [114], [115].

It is worth pointing out that the fundamental performance of a SG during faults hinges upon the capabilities of its AVR and the physical attributes of the generator, including machine constants and time constants. Maintaining the field excitation of the SG enables the production of a voltage that sustains the supply of SC current at the affected location. Fig. 27 depicts the typical SC current response of a synchronous generator during fault conditions, highlighting the time-decaying characteristics subsequent to the initial high fault current contribution.

Additionally, note the diverse characteristics of the SC current, where the maximum instantaneous peak contribution emerges during the initial cycle immediately following the fault. Furthermore, observe the primary current contributions,

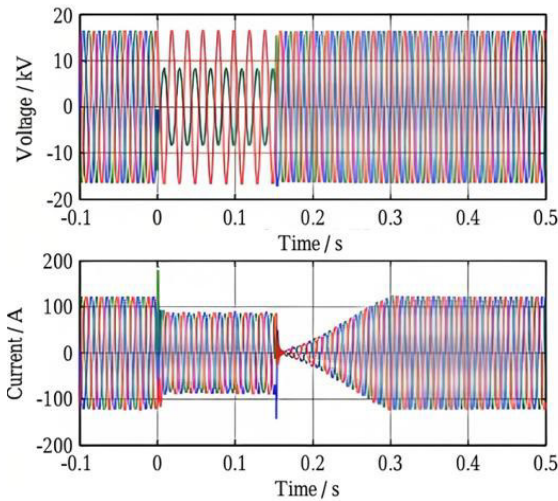


**FIGURE 24.** The fault response of a grid-connected PV system for a three-phase severe fault [111].

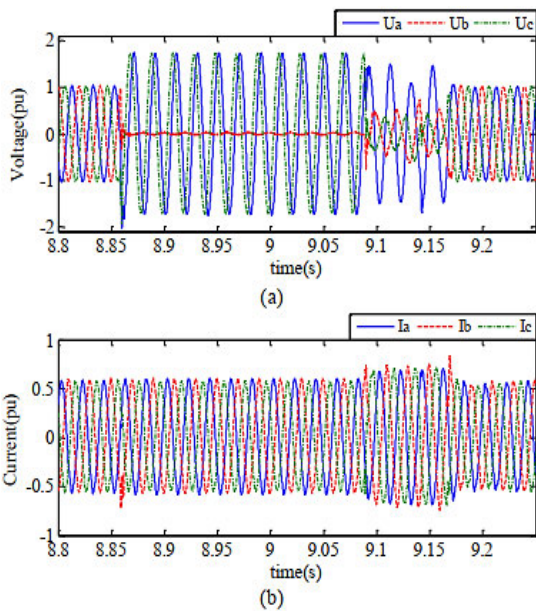


**FIGURE 25.** The fault response of a grid-connected PV to a single-phase to ground fault at 8.86 s, followed by a double-line to ground fault at 9.09 s: a) voltages b) currents [30].

which manifest as initial symmetrical and breaking symmetrical components as well. Note that Table 3, summarizes SC characteristics, modeling approaches, and the influencing factors of fully converter-interfaced sources (Types IV, V wind sources, and PV systems).

## VI. IMPACT OF INCREASED LARGE-SCALE PV AND WIND ON FAULT LEVEL

As discussed earlier in this paper, most of modern RESs are employing converter interfaces either partially (Type-3 wind) or fully (e.g., PV and Type-4 wind) when integrated to the electric grid. As such sources show limited and distinct SC characteristics and fault current contributions, it is

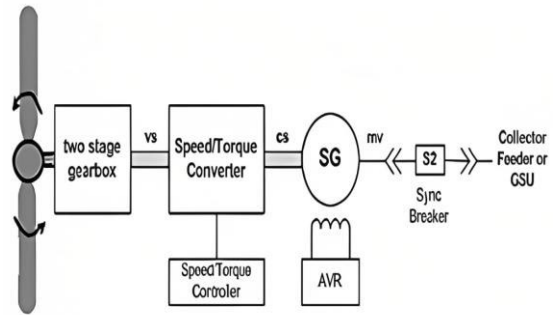


**FIGURE 26.** Typical configuration of wind generator (type-V) [113].

expected the fault level in modern and future power systems to be impacted in unconventional ways. This effect would be more pronounced when increased penetration of RESs are accompanied with displacement of large SGs, which is taking place currently in most power system across the world. This necessitates the need for better understanding the impact of high share of PE- connected RES on the fault level at both the transmission and distribution systems [15].

### A. NEW SC CHARACTERISTICS AND REDUCED FAULT LEVEL

The extensive integration of large PV and wind energy sources at the transmission level is replacing SGs, which traditionally provided the major fault current system during a fault to support the grid. This in turn reduces the fault level in the entire system and as a result, lower Short Circuit Ratio (SCR) in future power systems is expected [14], [116], [117], [118], [119], [120]. Researchers and system operators in many countries have been concerned regarding this issue and highlighted how important to examine the effect of high penetration of RESs on system dynamics and fault level. The studies in [73] and [116], have analyzed several scenarios of high penetration of PE-based RES generation and shown that a reduced fault level is likely expected. Also, a new method that formulates the correlation existing between the fault level and the high penetration of RESs has been proposed in those studies. Fig. 28 shows the impact of the increasing RESs' penetration (e.g., type-IV wind) on the fault level using the IEEE 39-bus test system.

According to another study conducted in [119], the increased penetration of nonsynchronous generators (e.g., RESs), would lead to operate power systems with low fault level which in its turn might limit the maximum penetration of such devices in the British power grid. Recent reports from the national grid system operator in UK, have pointed to the challenge of declining fault level in future power networks due to the high share of converter interfaced RESs. According to reports, the fault level is expected to experience a continuous decrease in future scenarios due to the rising penetration of RESs and the decommissioning of One of the main challenges associated with operating power systems with low fault level is represented by the reduced system strength [61],

**TABLE 3. Summarized fault characteristics, modeling, and influencing factors of PV systems, and Type IV and Type V wind sources.**

Attribute	Type-IV Wind (Full Power Converter Wind)	PV Systems	Type-V Wind (Mechanical Torque Converter-Interfaced Source)
<b>Grid Interface</b>	<ul style="list-style-type: none"> <li>- Fully converter-interfaced.</li> <li>- Generator is isolated from the grid via a fully-rated converter.</li> </ul>	<ul style="list-style-type: none"> <li>- Fully converter-interfaced.</li> <li>- Panels are linked via a DC/DC boost converter and a DC/AC inverter.</li> </ul>	<ul style="list-style-type: none"> <li>- Mechanical torque converter-interfaced.</li> <li>- Synchronous Generator is directly connected to the grid via a synchronizing breaker.</li> </ul>
<b>Fault Modeling Approach</b>	<ul style="list-style-type: none"> <li>- Controlled current source.</li> <li>- Output is dictated by the grid-side converter's control algorithms.</li> </ul>	<ul style="list-style-type: none"> <li>- Controlled current source (Similar to Type-IV wind).</li> <li>- Output is dictated by the grid-side converter's control algorithms.</li> </ul>	<ul style="list-style-type: none"> <li>- Standard Synchronous Generator (SG) modeling based on machine constants, time constants, and AVR capabilities.</li> </ul>
<b>Fault Current Contribution</b>	<ul style="list-style-type: none"> <li>- Initial Transient overshoot potentially up to 3 p.u.</li> <li>- Steady-state restricted to 1.1–1.6 p.u. (typically 1.1 p.u.)</li> </ul>	<ul style="list-style-type: none"> <li>- Fast transient (limited to ~2 p.u. or briefly higher).</li> <li>- Steady-state typically limited to 1.0–1.2 p.u. based on converter rating.</li> </ul>	<ul style="list-style-type: none"> <li>- High initial fault current followed by time-decaying characteristics.</li> <li>- Maximum peak contribution occurs in the first cycle.</li> </ul>
<b>Influencing Factors</b>	<ul style="list-style-type: none"> <li>- Manufacturer control strategy.</li> <li>- Inverter current limiters.</li> <li>- Voltage dip severity.</li> <li>- The LVRT <math>k</math>-factor.</li> </ul>	<ul style="list-style-type: none"> <li>- Inverter current limiters.</li> <li>- DC chopper activation.</li> <li>- The pre-fault operating conditions.</li> <li>- The LVRT <math>k</math>-factor.</li> </ul>	<ul style="list-style-type: none"> <li>- AVR capabilities.</li> <li>- Machine physical attributes (constants).</li> <li>- Maintenance of field excitation.</li> </ul>
<b>Remarks</b>	<ul style="list-style-type: none"> <li>- Often injects only positive sequence.</li> <li>- Unified response regardless of fault type.</li> </ul>	<ul style="list-style-type: none"> <li>- Minimal disparity in response between different fault types.</li> <li>- Response speed depends on fault detection/FRT.</li> </ul>	<ul style="list-style-type: none"> <li>- Mirrors standard SG behavior; maintains field excitation to sustain the supply of SC current</li> </ul>

[63]. The fault level is extensively utilized as an indicator characterizing the strength of power systems [121], [122]. SCR is also broadly used to indicate the system strength when it comes to the coupling points of RESs [59] SGs [123], [124]. Fig. 29 displays the average reduction in the fault level in the UK's national grid from 2019 to 2030 [124]. Conversely, the increased integration of RESs might result in changes to the conventional characteristics of SC currents [15], [21], [115]. For instance, the researchers in [15] have conducted sensitivity analysis of the SC characteristics in power systems with high RESs' penetration scenarios. The analysis has shown that the time-decaying response of the SC current, the initial fault current response, the instantaneous SC current, and the steady-state fault current components (see Fig. 27) would be pointedly affected by the penetration level of the RESs in the system. To be more specific, effects on these characteristics would be noticeable when the penetration of RESs surpasses certain levels in the grid. For instance, the study suggests an impact could be observed when RESs penetration exceeds 40%, though this threshold may differ depending on the composition and functioning of individual power systems.

Fig. 30 shows the SC characteristics of the fault current monitored on bus 9 in the IEEE 9-bus test system at different penetration levels of RESs (which is based on Type-IV wind generators) [15].

It can be noticed that the initial SC current is largely affected and reduced at both at 23% and 56% penetration

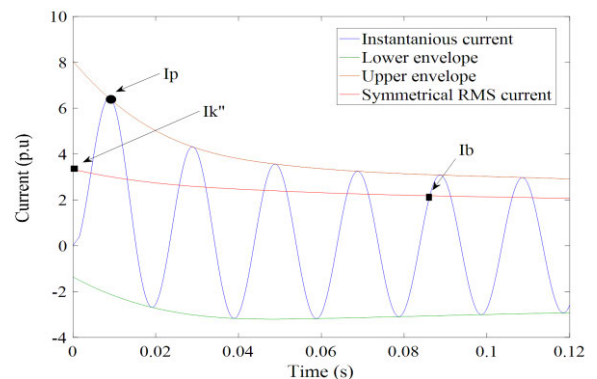


**FIGURE 27. Typical SC current contribution of SG and Type-V wind [15].**

scenarios. Also, it has been noticed that the steady-state component of the SC current has experienced a steady decline with the increased penetration of PE- connected RES, but less affected in compared to the initial SC current component. On the other hand, the level at which the SC current is decaying has also witnessed a serious change specially at the highest penetration scenario (i.e., 56% in that study).

**B. CHALLENGES AND NEGATIVE IMPLICATIONS OF NEW SC CHARACTERISTICS AND LOW FAULT LEVEL**

Lower fault levels and changes in the SC characteristics can potentially have negative implications on several aspects of

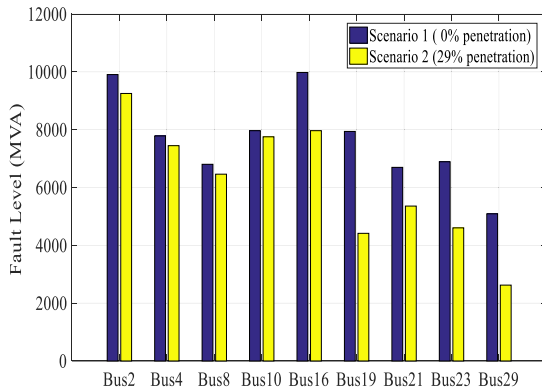


**FIGURE 28. Fault level Reduction due to 23% Penetration of Converter-based RESs in 39 bus test system [15].**

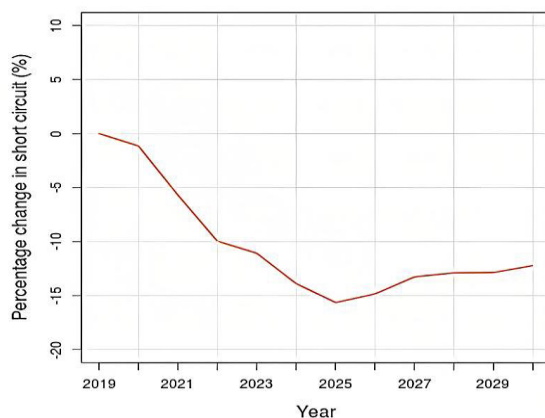


**FIGURE 29. UK National change in SC level from 2019-2030 [124].**

power systems. More specifically, in future power scenarios with high penetration of large-scale PV and wind generation. The main impact includes system strength, protection systems, and system stability.

### 1) SYSTEM STRENGTH

One of the main challenges associated with operating power systems with low fault level is represented by the reduced system strength [61], [63]. The fault level is extensively utilized as an indicator characterizing the strength of power systems [121], [122]. SCR is also broadly used to indicate system strength when it comes to the coupling points of RESs [59].

In vast majority of research available in literature, the term “system strength” is defined as the capability of the system to maintain the core characteristics when the system becomes altered from its normal state and subjected to disturbances such as SC events [14]. Although, the fault level might not be an accurate indicator to reflect the system strength in power systems with extensive penetration of RESs [61], the reduced fault level can still be representing a declined system strength. The fault level shortfall can also be understood as a higher impedance seen by a generator at a point of connection, which may cause more voltage sensitivity to disturbances.

This would require ensuring a minimum fault level in the systems specially at areas with high penetration of RESs is maintained to guarantee secure and safe grid operation [60]. According to the recent published reports, Australian Energy Market Operator (AEMO) and the Australian Energy Market Commission (AEMC), new rules have been set to manage the system strength and to ensure the required fault levels in the system. Such task has to be met by Transmission Network Service Providers and the System Strength Service Providers for each region [125].

### 2) SYSTEM PROTECTION

The alteration of SC characteristics and the reduced fault level have impacts on protection systems and protective relays. In classical power systems, where most of the power demand is met by the large central SGs, the settings for system protection have been set based on the well-understood SC response and the fault behavior of SGs.

Higher levels of fault current in such systems allow protection systems to achieve easily fault detection and isolation. However, such classical protection systems may face issues in terms of detection and responding to the faults due to the lower fault levels in high RESs penetration scenarios. For example, reduced and possibly delayed fault level response from PE-based RES may introduce a challenge to the transmission system protection performance [11], [126].

Moreover, the research presented in [127], has pointed to the possibility of failure of the lines distance protection due to the low fault level under high penetration of PE-based RESs. Also, it was reported that the dynamically varying source impedance under high penetration of RESs may cause the dynamic expansion of the mho circle to be unpredictable and inconsistent.

Researchers in [128], have reported to the importance of high fault level on the proper operation of transmission line distance protection. It was reported that transmission line protection using distance relays work by detecting fault impedance on the protected line or on nearby lines. The circuit breakers necessary to remove the fault are tripped by a relay if the impedance is measured of less than the actual impedance of a certain protected zone. This cannot be achieved without having adequate fault level providing enough fault current to the relay to function properly. Hence, if the fault level is reduced, meaning that inadequate available fault current, the relay may not operate as intended or may experience a delayed operation time.

On the other hand, over current protection might also get significantly affected by the reduced fault level and the delayed response of PE-based RES due to high penetration of such resources [10], [129]. In [129], the impact of the reduced fault level on the Over Current Relays (OCRs) operation, under high integration of PV systems penetration scenarios, has been investigated. Both the field-testing as well as the simulations have shown that a reduced fault level challenges the traditional method of fault analysis and the existing

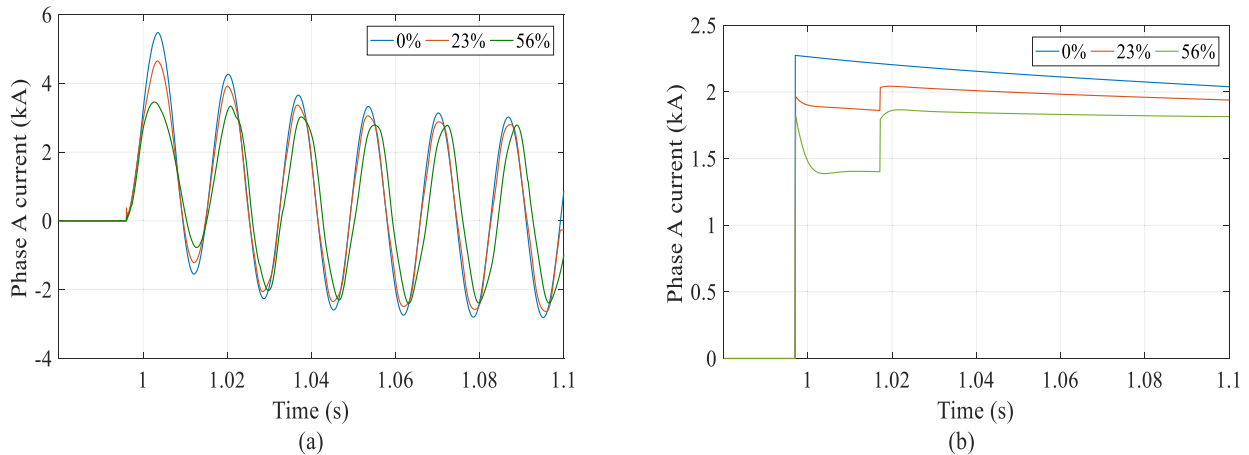


**FIGURE 30.** The SC current at different penetration levels of Converter-based RESs in 9-bus test system at bus 6 (a) Instantaneous current, (b) RMS current [73].

coordination of OCRs. The results have shown that OCRs would experience the problems of mis-operation and mal-operation.

Integration of RESs, especially on distribution networks, may cause a serious problem for the OCRs [10]. For instance, most of the feeders and lines experience bidirectional fault current flow because of the integration of large-scale RESs. Thus, those non-directional OCRs may not be able to protect these networks as planned. Another effect that can be observed is the impact of high PV penetration, which not only affects the current but also influences the triggering time reaction of protection relays. This might be due to the inability of the relays to distinguish between normal over currents, and faults based on the reduced SC current levels. Additionally, it is possible that the contribution of RESs to the SC current does not have enough negative- and zero-sequence currents for directional relays to function properly [10]. On the other hand, not only distance and overcurrent protection relays might be affected by the reduced fault levels due to higher penetration of PE-based RES, but also the differential protection may face challenges in their operation. For instance, the differential relays might not detect a very slight change between the currents in case of low fault level. Hence, it might be essential to set a relatively high bias to prevent malfunction [130].

### 3) SYSTEM STABILITY

Stability is somehow correlated to the previous aspects of system strength and protection system. Once the system strength and the proper operation of the system protection are ensured, the system stability would be improved. Traditionally, the high fault level contribution from SGs has played a key role in supporting the voltage stability [62]. This is due to the availability of the excitation current control which maintains the terminal voltage during the faulty conditions. Furthermore, SGs are directly and parallelly connected to the system, and their internal reactance influences the equivalent impedance

on the network from the generator's terminal to the faulty point. However, as the penetration of PV and wind generators increases, which predominantly utilize converter interfaces, the fault level is reduced, thereby negatively impacting voltage stability. In other words, the reduction in fault level could lead to the creation of weaker grids, which, in turn, may increase the likelihood of voltage collapse and voltage stability problems in the system [62], [122], [131].

One other important aspect of system stability is represented by the stable connection and operation of the RESs. For instance, for such resources to function reliably and stably, the system must have a certain amount of strength. At the RES's grid connection point, the SCR is frequently used to describe the system strength [132]. In operating these sources at the PCC with a reduced fault level can lead to decrease the SCR. It is typical to consider a connection of SCR of less than 3 as a weak connection (i.e., low SCR). Under such conditions, the RESs may face instability problems [133].

On the other hand, weak grid connections (i.e., low SCR) significantly affect the operation and stability of the HVDC lines, especially those that use line-commutated converters (LCC). The line voltage affects how these switches communicate with one another in this technology. As the voltage of the line voltage might be more susceptible to disturbances in case of weak-connection (i.e., very low SCR), ensuring a certain level of fault level is a crucial design factor. Low fault levels can potentially affect the operation of HVDC links negatively and may result in several problems, including voltage instability, frequency resonances, and overvoltage from load rejections [134], [135].

Moreover, the utilization of phase-locked loop (PLL) in RESs in order to get synchronized with the grid may suffer from instability issues [13], [136]. This is mostly caused by the voltage distortion that can happen in the event of disturbances in low fault level conditions. Hence, PLL would not be capable of operating stably which would result in

**TABLE 4. Summarized challenges and negative implications of new SC characteristics and low fault level on power systems.**

Area of Impact	System / Method Affected	Challenges and Negative Implications
System Strength	- Grid Strength Indicators (SCR/Fault Level)	- Reduced fault levels indicate lower system strength. - Leading to higher impedance at connection points. - Increased voltage sensitivity to disturbances.
System Protection	- Distance Protection	- Low fault levels can cause failure to trip or delayed operation. - Dynamically varying source impedance leads to unpredictable expansion of the mho circle.
	- Overcurrent Relays	- Traditional coordination is challenged. - Relays may experience mis-operation or mal-operation due to an inability to distinguish between normal and faulty currents.
	- Directional and Differential Relays	- Directional relays may fail due to a lack of negative/zero-sequence currents. - Differential relays require higher bias settings to prevent malfunction at low fault levels.
System Stability	- Voltage Stability Mechanisms	- Lower fault levels create "weaker" grids. - Significantly increasing the risk of voltage collapse and general voltage instability.
	- HVDC Links	- Low SCR makes HVDC links susceptible to commutation failures. - Frequency resonances. - Overvoltage during load rejections.
	- Phase-Locked Loops (PLL)	- Voltage distortions in low-fault conditions cause instability in synchronization. - Leading to poor tracking of grid frequency and phase.
Operation of RESs	- FRT & Grid Connection	- Sources operating at connection points with $SCR < 3$ (weak connections) face inherent instability problems during grid disturbances.

poor tracking of the grid frequency and grid voltage phase. Consequently, this may negatively impact the power transfer control between the RESs and the grid. Note that Table 4, summarizes the challenges and negative implications of the new SC characteristics and low fault level discussed above.

**VII. CONCLUSION**

In this paper, we have delved into fault level considerations in future power scenarios characterized by high penetration of RESs, with a focus on PV and wind generation. At first, the paper provided a deep insight on the global trends of RESs integration focusing on the global figures on the advancements in the utilization of PV and wind technologies. Then, the study examined fault levels and SC currents characteristics in classical power systems reliant on SGs. Subsequently, we explored grid codes and FRT requirements governing SC signatures and the behavior of different PV and wind generation during faults. To differentiate between fault current contributions based on technology and grid interface methods, we categorized power-electronic-based RESs into four groups. These include directly connected sources without converter interfaces, partially converter-interfaced sources, fully converter-interfaced sources, and mechanical torque converter-interfaced sources.

Our analysis extended to dissecting the impact of increased penetration of such generation on SC characteristics and fault levels. Furthermore, we discussed the implications and negative repercussions of altered SC characteristics, coupled with diminished fault levels, on power system operation. This encompassed aspects such as system strength, protection, and stability.

The findings of the paper highlight the varied and constrained SC currents contributions from PV and wind RESs when compared to SGs. The factors might influence the SC current contributions from PV and different wind types such as grid codes; FRT control and the utilization of converter interfaces have been comprehensively described. One more significant finding of this study is represented by the alteration of traditional SC characteristics and a substantial reduction in fault levels when large central SGs are displaced by such RESs. Consequently, not only does system strength deteriorate, but system protection and stability are also affected in non-traditional ways. Our extensive review emphasizes the seriousness of these challenges the necessity need for more considerations as PV and wind RESs would become the primary energy sources for the grid. The analyses presented a clear warning, highlighting the urgent need for mitigation measures to address the challenges stemming from altered SC characteristics and reduced fault levels in future scenarios.

## REFERENCES

- [1] M. Victoria, N. Haegel, I. M. Peters, R. Sinton, A. Jäger-Waldau, C. del Cañizo, C. Breyer, M. Stocks, A. Blakers, I. Kaizuka, K. Komoto, and A. Smets, "Solar photovoltaics is ready to power a sustainable future," *Joule*, vol. 5, no. 5, pp. 1041–1056, May 2021.
- [2] D. Gielen, F. Boshell, D. Saygin, M. D. Bazilian, N. Wagner, and R. Gorini, "The role of renewable energy in the global energy transformation," *Energy Strategy Rev.*, vol. 24, pp. 38–50, Apr. 2019.
- [3] (2021). *Renewables 2021 Global Status Report*. [Online]. Available: <https://www.ren21.net/reports/global-status-report/>
- [4] B. Kroposki, B. Johnson, Y. Zhang, V. Gevorgian, P. Denholm, B.-M. Hodge, and B. Hannegan, "Achieving a 100% renewable grid: Operating electric power systems with extremely high levels of variable renewable energy," *IEEE Power Energy Mag.*, vol. 15, no. 2, pp. 61–73, Mar. 2017.
- [5] (2016). *Renewables 2016: Global Status Report*. [Online]. Available: [https://inis.iaea.org/search/search.aspx?orig\\_q=RN:47082519](https://inis.iaea.org/search/search.aspx?orig_q=RN:47082519)
- [6] M. Z. Jacobson and M. A. Delucchi, "Providing all global energy with wind, water, and solar power, part I: Technologies, energy resources, quantities and areas of infrastructure, and materials," *Energy Policy*, vol. 39, no. 3, pp. 1154–1169, Mar. 2011.
- [7] M. Z. Jacobson et al., "100% clean and renewable wind, water, and sunlight all-sector energy roadmaps for 139 countries of the world," *Joule*, vol. 1, no. 1, pp. 108–121, 2017.
- [8] P. Rahdan, E. Zeyen, C. Gallego-Castillo, and M. Victoria, "Distributed photovoltaics provides key benefits for a highly renewable European energy system," *Appl. Energy*, vol. 360, Apr. 2024, Art. no. 122721.
- [9] K. Guerra, P. Haro, R. E. Gutiérrez, and A. Gómez-Barea, "Facing the high share of variable renewable energy in the power system: Flexibility and stability requirements," *Appl. Energy*, vol. 310, Mar. 2022, Art. no. 118561.
- [10] V. Telukunta, J. Pradhan, A. Agrawal, M. Singh, and S. G. Srivani, "Protection challenges under bulk penetration of renewable energy resources in power systems: A review," *CSEE J. Power Energy Syst.*, vol. 3, no. 4, pp. 365–379, Dec. 2017.
- [11] R. Li, C. Booth, A. Dysko, A. Roscoe, H. Urdal, and J. Zhu, "Protection challenges in future converter dominated power systems: Demonstration through simulation and hardware tests," in *Proc. Int. Conf. Renew. Power Gener. (RPG)*, Oct. 2015, pp. 1–6.
- [12] V. R. Vakacharla, K. Gnana, P. Xuewei, B. L. Narasimharaju, M. Bhukya, A. Banerjee, R. Sharma, and A. K. Rathore, "State-of-the-art power electronics systems for solar-to-grid integration," *Sol. Energy*, vol. 210, pp. 128–148, Nov. 2020.
- [13] R. Aljarrah, B. B. Fawaz, Q. Salem, M. Karimi, H. Marzooghi, and R. Azizpanah-Abarghoee, "Issues and challenges of grid-following converters interfacing renewable energy sources in low inertia systems: A review," *IEEE Access*, vol. 12, pp. 5534–5561, 2024, doi: 10.1109/ACCESS.2024.3349630.
- [14] S. Gordon, K. Bell, and Q. Hong, "Implications of reduced fault level and its relationship to system strength: A Scotland case study," in *Proc. CIGRE Session*, 2022, pp. 1–10.
- [15] R. Aljarrah, H. Marzooghi, J. Yu, and V. Terzija, "Sensitivity analysis of transient short circuit current response to the penetration level of non-synchronous generation," *Int. J. Electr. Power Energy Syst.*, vol. 125, Feb. 2021, Art. no. 106556.
- [16] R. Aljarrah, H. Marzooghi, and V. Terzija, "Mitigating the impact of fault level shortfall in future power systems with high penetration of converter-interfaced renewable energy sources," *Int. J. Electr. Power Energy Syst.*, vol. 149, Jul. 2023, Art. no. 109058.
- [17] S. Impram, S. Varbak Nese, and B. Oral, "Challenges of renewable energy penetration on power system flexibility: A survey," *Energy Strategy Rev.*, vol. 31, Sep. 2020, Art. no. 100539.
- [18] D. Turcotte and F. Katiraei, "Fault contribution of grid-connected inverters," in *Proc. IEEE Electr. Power Energy Conf. (EPEC)*, Oct. 2009, pp. 1–5.
- [19] J. Keller, B. Kroposki, R. Bravo, and S. Robles, "Fault current contribution from single-phase PV inverters," in *Proc. 37th IEEE Photovoltaic Specialists Conf.*, Jun. 2011, pp. 001822–001826.
- [20] R. Walling et al., "Fault current contributions from wind plants," in *Proc. 68th Annu. Conf. Protective Relay Eng.*, 2015, pp. 137–227, doi: 10.1109/CPRE.2015.7102165.
- [21] C. A. Plet, M. Graovac, T. C. Green, and R. Iravani, "Fault response of grid-connected inverter dominated networks," in *Proc. IEEE PES Gen. Meeting*, Jul. 2010, pp. 1–8.
- [22] O. Anaya-Lara, X. Wu, P. Cartwright, J. B. Ekanayake, and N. Jenkins, "Performance of doubly fed induction generator (DFIG) during network faults," *Wind Eng.*, vol. 29, no. 1, pp. 49–66, Jan. 2005.
- [23] T. Sobhy, N. Hemdan, M. Hamada, and M. Wahab, "German grid code aspects discussion: Low voltage ride-through of converter based decentralized generation," *Int. J. Distrib. Energy Resour. Smart Grids*, vol. 11, pp. 129–141, Oct. 2015.
- [24] C. Sourkounis and P. Tourou, "Grid code requirements for wind power integration in Europe," in *Proc. Conf. Papers Sci.*, vol. 2013, 2013, pp. 1–9.
- [25] (2022). *Grid Codes for Renewable Powered Systems*. [Online]. Available: [https://www.irena.org/publications/2022/Apr/](https://www.irena.org/publications/2022/Apr/Grid-codes-for-renewable-powered-systems) Grid-codes-for-renewable-powered-systems
- [26] TenneT TSO GmbH. (2022). *Grid Connection Requirements-High and Extra-High Voltage*. [Online]. Available: <https://www.tennet.eu/grid-connection-regulations>
- [27] J. Morren. (2006). *Grid Support By Power Electronic Converters of Distributed Generation Units*. [Online]. Available: <https://www.osti.gov/etdweb/biblio/21461678>
- [28] Y.-K. Wu, S.-M. Chang, and P. Mandal, "Grid-connected wind power plants: A survey on the integration requirements in modern grid codes," *IEEE Trans. Ind. Appl.*, vol. 55, no. 6, pp. 5584–5593, Nov. 2019.
- [29] A. Stankovic, D. Schreiber, and X. Zheng, "Grid-fault ride-through control method for a wind turbine inverter," in *Smart Power Grids 2011*. Cham, Switzerland: Springer, 2012, pp. 543–563.
- [30] S. Vijayakumar and U. Shenoy, "Behavior of photovoltaic system during grid disturbances," M.S. thesis, Indian Inst. Sci., Bengaluru, India, 2012.
- [31] N. Samaan, R. Zavadil, J. Charles Smith, and J. Conto, "Modeling of wind power plants for short circuit analysis in the transmission network," in *Proc. IEEE/PES Transmiss. Distrib. Conf. Expo.*, Apr. 2008, pp. 1–7.
- [32] M. Chaudhary, S. M. Brahma, and S. J. Ranade, "Short circuit analysis of type II induction generator and wind farm," in *Proc. PES T&D*, May 2012, pp. 1–5.
- [33] E. Muljadi, N. Samaan, V. Gevorgian, J. Li, and S. Pasupulati, "Short circuit current contribution for different wind turbine generator types," in *Proc. IEEE PES Gen. Meeting*, Jul. 2010, pp. 1–8.
- [34] R. J. Nelson, "Short-circuit contributions of full converter wind turbines," in *Proc. PES T&D*, May 2012, pp. 1–5.
- [35] Y. Yuan and F. Wu, "Short-circuit current analysis for DFIG wind farm considering the action of a crowbar," *Energies*, vol. 11, no. 2, p. 425, Feb. 2018.
- [36] E. Farantatos, U. Karaagac, H. Saad, and J. Mahseredjian, "Short-circuit current contribution of converter interfaced wind turbines and the impact on system protection," in *Proc. IREP Symp. Bulk Power Syst. Dyn. Control-IX Optim., Secur. Control Emerg. Power Grid*, Aug. 2013, pp. 1–9.
- [37] S. Wang, N. Chen, D. Yu, A. Foley, L. Zhu, K. Li, and J. Yu, "Flexible fault ride through strategy for wind farm clusters in power systems with high wind power penetration," *Energy Convers. Manage.*, vol. 93, pp. 239–248, Mar. 2015.
- [38] N. Nimpitiwan, G. T. Heydt, R. Ayyanar, and S. Suryanarayanan, "Fault current contribution from synchronous machine and inverter based distributed generators," *IEEE Trans. Power Del.*, vol. 22, no. 1, pp. 634–641, Jan. 2007.
- [39] S. Liu, T. Bi, and Y. Liu, "Theoretical analysis on the short-circuit current of inverter-interfaced renewable energy generators with fault-ride-through capability," *Sustainability*, vol. 10, no. 1, p. 44, Dec. 2017.
- [40] C. Feltes. (2012). *Advanced Fault Ride-Through Control of DFIG Based Wind Turbines Including Grid Connection Via VSC-HVDC*. [Online]. Available: <https://www.osti.gov/etdweb/biblio/21573518>
- [41] R. Hiremath and T. Moger, "Comprehensive review on low voltage ride through capability of wind turbine generators," *Int. Trans. Electr. Energy Syst.*, vol. 30, no. 10, p. 12524, Oct. 2020.
- [42] W. Chen, T. Zheng, and J. Han, "Fault characteristic and low voltage ride-through requirements applicability analysis for a permanent magnet synchronous generator-based wind farm," *Energies*, vol. 12, no. 17, p. 3400, Sep. 2019.

- [43] J. Fortmann, R. Pfeiffer, E. Haesen, F. van Hulle, F. Martin, H. Urdal, and S. Wachtel, "Fault-ride-through requirements for wind power plants in the ENTSO-E network code on requirements for generators," *IET Renew. Power Gener.*, vol. 9, no. 1, pp. 18–24, Jan. 2015.
- [44] B. Weise, "Impact of K-factor and active current reduction during fault-ride-through of generating units connected via voltage-sourced converters on power system stability," *IET Renew. Power Gener.*, vol. 9, no. 1, pp. 25–36, Jan. 2015.
- [45] M. Nadour, A. Essadki, and T. Nasser, "Improving low-voltage ride-through capability of a multimegawatt DFIG based wind turbine under grid faults," *Protection Control Mod. Power Syst.*, vol. 5, no. 1, pp. 1–13, Dec. 2020.
- [46] M. Curzi, R. Sharma, and F. Martin, "In fault ride through reactive current rise time requirements of various European grid codes—Analysis based on a full-converter wind turbine," *Wind Energy*, vol. 19, no. 6, pp. 1121–1133, Jun. 2016.
- [47] C.-T. Lee, C.-W. Hsu, and P.-T. Cheng, "A low-voltage ride-through technique for grid-connected converters of distributed energy resources," *IEEE Trans. Ind. Appl.*, vol. 47, no. 4, pp. 1821–1832, Jul. 2011.
- [48] M. Tarafdar Hagh and T. Khalili, "A review of fault ride through of PV and wind renewable energies in grid codes," *Int. J. Energy Res.*, vol. 43, no. 4, pp. 1342–1356, Mar. 2019.
- [49] S. B. Naderi, P. Davari, D. Zhou, M. Negnevitsky, and F. Blaabjerg, "A review on fault current limiting devices to enhance the fault ride-through capability of the doubly-fed induction generator based wind turbine," *Appl. Sci.*, vol. 8, no. 11, p. 2059, Oct. 2018.
- [50] B. Mahamedi, M. Eskandari, J. E. Fletcher, and J. Zhu, "Sequence-based control strategy with current limiting for the fault ride-through of inverter-interfaced distributed generators," *IEEE Trans. Sustain. Energy*, vol. 11, no. 1, pp. 165–174, Jan. 2020.
- [51] P. Makolo, R. Zamora, and T.-T. Lie, "The role of inertia for grid flexibility under high penetration of variable renewables—A review of challenges and solutions," *Renew. Sustain. Energy Rev.*, vol. 147, Sep. 2021, Art. no. 111223.
- [52] S. Saha, M. Saleem, and T. Roy, "Impact of high penetration of renewable energy sources on grid frequency behavior," *Int. J. Electr. Power Energy Syst.*, vol. 145, Feb. 2023, Art. no. 108701.
- [53] Y. Cheng, R. Azizipannah-Abarghoosee, S. Azizi, L. Ding, and V. Terzija, "Smart frequency control in low inertia energy systems based on frequency response techniques: A review," *Appl. Energy*, vol. 279, Dec. 2020, Art. no. 115798.
- [54] S. Homan, N. Mac Dowell, and S. Brown, "Grid frequency volatility in future low inertia scenarios: Challenges and mitigation options," *Appl. Energy*, vol. 290, May 2021, Art. no. 116723.
- [55] M. N. H. Shazon, Nahid-Al-Masood, and A. Jawad, "Frequency control challenges and potential countermeasures in future low-inertia power systems: A review," *Energy Rep.*, vol. 8, pp. 6191–6219, Nov. 2022.
- [56] C. Mosca, F. Arrigo, A. Mazza, E. Bompard, E. Carpaneto, G. Chicco, and P. Cuccia, "Mitigation of frequency stability issues in low inertia power systems using synchronous compensators and battery energy storage systems," *IET Gener., Transmiss. Distrib.*, vol. 13, no. 17, pp. 3951–3959, Sep. 2019.
- [57] J. Shair, H. Li, J. Hu, and X. Xie, "Power system stability issues, classifications and research prospects in the context of high-penetration of renewables and power electronics," *Renew. Sustain. Energy Rev.*, vol. 145, Jul. 2021, Art. no. 111111.
- [58] R. Shah, N. Mithulananthan, R. C. Bansal, and V. K. Ramachandaramurthy, "A review of key power system stability challenges for large-scale PV integration," *Renew. Sustain. Energy Rev.*, vol. 41, pp. 1423–1436, Jan. 2015.
- [59] D. Wu, G. Li, M. Javadi, A. M. Malysheff, M. Hong, and J. N. Jiang, "Assessing impact of renewable energy integration on system strength using site-dependent short circuit ratio," *IEEE Trans. Sustain. Energy*, vol. 9, no. 3, pp. 1072–1080, Jul. 2018.
- [60] L. Yu, K. Meng, W. Zhang, and Y. Zhang, "An overview of system strength challenges in Australia's national electricity market grid," *Electronics*, vol. 11, no. 2, p. 224, Jan. 2022.
- [61] R. Aljarrah, M. Karimi, H. Marzooghi, S. Alnaser, M. Al-Omary, Q. Saleem, and S. Harasis, "Relationship between fault level and system strength in future renewable-rich power grids," *Appl. Sci.*, vol. 13, no. 1, p. 142, Dec. 2022.
- [62] M. G. Dozein, P. Mancarella, T. K. Saha, and R. Yan, "System strength and weak grids: Fundamentals, challenges, and mitigation strategies," in *Proc. Australas. Universities Power Eng. Conf. (AUPEC)*, Nov. 2018, pp. 1–7.
- [63] H. Urdal, R. Ierna, J. Zhu, C. Ivanov, A. Dahresobh, and D. Rostom, "System strength considerations in a converter dominated power system," *IET Renew. Power Gener.*, vol. 9, no. 1, pp. 10–17, Jan. 2015.
- [64] D. V. Pombo, J. Martinez-Rico, and H. M. Marcinkowski, "Towards 100% renewable islands in 2040 via generation expansion planning: The case of São vicente, Cape Verde," *Appl. Energy*, vol. 315, Jun. 2022, Art. no. 118869.
- [65] (2022). *Renewable Capacity Highlights*. [Online]. Available: <https://www.irena.org/Publications>
- [66] (2022). *Renewables 2022 Global Status Report United States of America Factsheet*. [Online]. Available: <https://policycommons.net/>
- [67] N. Haegel and S. Kurtz, "Global progress toward renewable electricity: Tracking the role of solar," *IEEE J. Photovolt.*, vol. 11, no. 6, pp. 1335–1342, Nov. 2021.
- [68] M. Karimi, H. Mokhlis, K. Naidu, S. Uddin, and A. H. A. Bakar, "Photovoltaic penetration issues and impacts in distribution network—A review," *Renew. Sustain. Energy Rev.*, vol. 53, pp. 594–605, Jan. 2016.
- [69] (2022). *Wind Energy in Europe: 2021 Statistics and the Outlook for 2022-2026*. [Online]. Available: <https://windeurope.org/>
- [70] (2022). *GLOBAL WIND REPORT 2022*. [Online]. Available: <https://gwec.net/global-wind-report-2022/>
- [71] T. Nagsarkar and M. Sukhija, *Power Systems Analysis*. London, U.K.: Oxford Univ. Press, 2007.
- [72] N. Tleis, *Power systems modeling and fault analysis: Theory and practice*. Elsevier, 2007.
- [73] R. R. Aljarrah, "Assessment of fault level in power systems with high penetration of non-synchronous generation," Ph.D. dissertation, Univ. Manchester, Manchester, U.K., 2020.
- [74] L. Huang, J. Xu, Y. Sun, M. Chen, and H. Xu, "Voltage stability analysis and monitoring based on short circuit capacity," in *Proc. IEEE Int. Conf. Power Syst. Technol. (POWERCON)*, Oct. 2012, pp. 1–5.
- [75] D. Babazadeh, A. Muthukrishnan, L. Nordström, P. Mitra, and T. Larsson, "Short circuit capacity estimation for HVDC control application," in *Proc. Power Syst. Comput. Conf. (PSCC)*, Jun. 2016, pp. 1–7.
- [76] F. Zhang, H. Xin, D. Wu, Z. Wang, and D. Gan, "Assessing strength of multi-infeed LCC-HVDC systems using generalized short-circuit ratio," *IEEE Trans. Power Syst.*, vol. 34, no. 1, pp. 467–480, Jan. 2019.
- [77] I. Kasicki, *Short Circuits in Power Systems: A Practical Guide to IEC 60909-0*. Hoboken, NJ, USA: Wiley, 2018.
- [78] A. Q. Al-Shetwi, M. Z. Sujod, F. Blaabjerg, and Y. Yang, "Fault ride-through control of grid-connected photovoltaic power plants: A review," *Sol. Energy*, vol. 180, pp. 340–350, Mar. 2019.
- [79] M. Tsili and S. Papathanassiou, "A review of grid code technical requirements for wind farms," *IET Renew. Power Gener.*, vol. 3, no. 3, pp. 308–332, Sep. 2009.
- [80] M. Mohseni and S. M. Islam, "Review of international grid codes for wind power integration: Diversity, technology and a case for global standard," *Renew. Sustain. Energy Rev.*, vol. 16, no. 6, pp. 3876–3890, Aug. 2012.
- [81] Z. Hassan, A. Amir, J. Selvaraj, and N. A. Rahim, "A review on current injection techniques for low-voltage ride-through and grid fault conditions in grid-connected photovoltaic system," *Sol. Energy*, vol. 207, pp. 851–873, Sep. 2020.
- [82] (2013). *Requirements for Grid Connection Applicable To All Generators*. [Online]. Available: [https://www.entsoe.eu/network\\_codes/rfg/](https://www.entsoe.eu/network_codes/rfg/)
- [83] S. Marmouh, M. Boutoubat, L. Mokrani, and M. Machmoum, "A coordinated control and management strategy of a wind energy conversion system for a universal low-voltage ride-through capability," *Int. Trans. Electr. Energy Syst.*, vol. 29, no. 8, p. 12035, Aug. 2019.
- [84] J. Jia, G. Yang, and A. H. Nielsen, "A review on grid-connected converter control for short-circuit power provision under grid unbalanced faults," *IEEE Trans. Power Del.*, vol. 33, no. 2, pp. 649–661, Apr. 2018.
- [85] F. Iov, A. D. Hansen, P. E. Sørensen, and N. A. Cutululis, "Mapping of grid faults and grid codes," Risø National Laboratory, Tech. Rep., 2007.
- [86] I. Jorge, H. Pinheiro, and H. Abilio, "Wind turbines reactive current control during unbalanced voltage dips," in *Modeling and Control Aspects of Wind Power Systems*, 2013, p. 61.

- [87] A. Q. Al-Shetwi, M. Z. Sujod, F. Blaabjerg, and Y. Yang, "Fault ride-through control of grid-connected photovoltaic power plants: A review," *Sol. Energy*, vol. 180, pp. 340–350, Mar. 2019.
- [88] B. Chen, A. Shrestha, F. A. Ituzaro, and N. Fischer, "Addressing protection challenges associated with type 3 and type 4 wind turbine generators," in *Proc. 68th Annu. Conf. Protective Relay Eng.*, Mar. 2015, pp. 335–344.
- [89] A. Hooshyar, M. A. Azzouz, and E. F. El-Saadany, "Distance protection of lines emanating from full-scale converter-interfaced renewable energy power plants—Part I: Problem statement," *IEEE Trans. Power Del.*, vol. 30, no. 4, pp. 1770–1780, Aug. 2015.
- [90] M. T. Villén, M. P. Comech, E. M. Carrasco, and A. A. P. Hurtado, "Influence of negative sequence injection strategies on faulted phase selector performance," *Energies*, vol. 15, no. 16, p. 6018, Aug. 2022.
- [91] J. A. Baroudi, V. Dinavahi, and A. M. Knight, "A review of power converter topologies for wind generators," *Renew. Energy*, vol. 32, no. 14, pp. 2369–2385, Nov. 2007.
- [92] (2020). *Wind Energy Generation Systems -Part 27-1: Electrical Simulation Models - Generic Models*. [Online]. Available: <https://webstore.iec.ch/publication/32564>
- [93] T. Ackermann, *Wind Power in Power Systems*. Hoboken, NJ, USA: Wiley, 2012.
- [94] E. Muljadi, N. Samaan, V. Gevorgian, J. Li, and S. Pasupulati, "Different factors affecting short circuit behavior of a wind power plant," *IEEE Trans. Ind. Appl.*, vol. 49, no. 1, pp. 284–292, Jan. 2013.
- [95] D. F. Howard, J. Restrepo, T. Smith, M. Starke, J. Dang, and R. G. Harley, "Calculation of fault current contribution of type i wind turbine-generators," in *Proc. IEEE Power Energy Soc. Gen. Meeting*, Jul. 2011, pp. 1–7.
- [96] M. Osman, N. Segal, A. Najafzadeh, and J. Harris, "Short-circuit modeling and system strength," North Amer. Electr. Rel. Corp., Atlanta, GA, USA, White Paper, 2018.
- [97] A. El-Naggar and I. Erlich, "Analysis of fault current contribution of doubly-fed induction generator wind turbines during unbalanced grid faults," *Renew. Energy*, vol. 91, pp. 137–146, Jun. 2016.
- [98] F. Blaabjerg and K. Ma, "Future on power electronics for wind turbine systems," *IEEE J. Emerg. Sel. Topics Power Electron.*, vol. 1, no. 3, pp. 139–152, Sep. 2013.
- [99] Y. Chang, J. Hu, G. Song, X. Kong, and Y. Yuan, "Impact of DFIG-based wind turbine's fault current on distance relay during symmetrical faults," *IET Renew. Power Gener.*, vol. 14, no. 16, pp. 3097–3102, 2020.
- [100] S. Müller, M. Deicke, and R. Doncker, "Doubly fed induction generator systems for wind turbines," *IEEE Ind. Appl. Mag.*, vol. 8, no. 3, pp. 26–33, Mar. 2002.
- [101] G. Iwanski and W. Koczara, "DFIG-based power generation system with UPS function for variable-speed applications," *IEEE Trans. Ind. Electron.*, vol. 55, no. 8, pp. 3047–3054, Aug. 2008.
- [102] J. Ouyang, D. Zheng, X. Xiong, C. Xiao, and R. Yu, "Short-circuit current of doubly fed induction generator under partial and asymmetrical voltage drop," *Renew. Energy*, vol. 88, pp. 1–11, Apr. 2016.
- [103] W. Xu, Y. Li, C. Liu, and C. Lv, "Practical calculation model for short-circuit current of doubly fed induction generator in large power grids," in *Proc. IET Conf.*, 2024, pp. 13–25.
- [104] P. Karaliolios, A. Ishchenko, E. Coster, J. Myrzik, and W. Kling, "Overview of short-circuit contribution of various distributed generators on the distribution network," in *Proc. 43rd Int. Universities Power Eng. Conf.*, Sep. 2008, pp. 1–6.
- [105] R. A. Walling, E. Gursoy, and B. English, "Current contributions from type 3 and type 4 wind turbine generators during faults," in *Proc. IEEE Power Energy Soc. Gen. Meeting*, Jul. 2011, pp. 1–6.
- [106] E. Camm et al., "Characteristics of wind turbine generators for wind power plants," in *Proc. IEEE Power Energy Soc. Gen. Meeting*, 2009, pp. 1–5.
- [107] T. Bi, B. Yang, K. Jia, L. Zheng, Q. Liu, and Q. Yang, "Review on renewable energy source fault characteristics analysis," *CSEE J. Power Energy Syst.*, vol. 8, no. 4, pp. 963–972, Jul. 2022.
- [108] M. Bradt, M. R. Behnke, W. G. Bloethe, C. Brooks, E. H. Camm, W. Dilling, B. Goltz, J. Li, J. Niemira, K. Nuckles, J. Patiflo, M. Reza, B. Richardson, N. Samaan, J. Schoene, T. Smith, I. Snyder, M. Starke, R. Walling, and G. Zahalka, "Wind plant collector system fault protection and coordination," in *Proc. IEEE PES T&D*, Apr. 2010, pp. 1–5.
- [109] M. Ndreko, M. Popov, A. A. van der Meer, and M. A. M. van der Meijden, "The effect of the offshore VSC-HVDC connected wind power plants on the unbalanced faulted behavior of AC transmission systems," in *Proc. IEEE Int. Energy Conf. (ENERGYCON)*, Apr. 2016, pp. 1–6.
- [110] S. Liu, H. Zhang, P. Zhang, Z. Li, and Z. Wang, "Equivalent model of photovoltaic power station considering different generation Units' fault current contributions," *Energies*, vol. 15, no. 1, p. 229, Dec. 2021.
- [111] T. Neumann and I. Erlich, "Short circuit current contribution of a photovoltaic power plant," *IFAC Proc. Volumes*, vol. 45, no. 21, pp. 343–348, 2012.
- [112] A. Bracale, P. Caramia, G. Carpinelli, and A. R. Di Fazio, "Modeling the three-phase short-circuit contribution of photovoltaic systems in balanced power systems," *Int. J. Electr. Power Energy Syst.*, vol. 93, pp. 204–215, Dec. 2017.
- [113] J. Schlabbach, *Short-Circuit Currents*. London, U.K.: Institution of Electrical Engineers (IET), 2005.
- [114] *Short-Circuit Currents in Three-Phase Ac Systems, Part 0: Calculation of Currents*, IEC, Geneva, Switzerland, 2016.
- [115] R. Aljarrah, H. Marzooghi, V. Terzija, and J. Yu, "Issues and challenges of steady-state fault calculation methods in power systems with a high penetration of non-synchronous generation," in *Proc. IEEE Milan PowerTech*, Jun. 2019, pp. 1–6.
- [116] R. Aljarrah, H. Marzooghi, J. Yu, and V. Terzija, "Monitoring of fault level in future grid scenarios with high penetration of power electronics-based renewable generation," *IET Gener., Transmiss. Distrib.*, vol. 15, no. 2, pp. 294–305, Jan. 2021.
- [117] S. Hadavi, M. Z. Mansour, and B. Bahrani, "Optimal allocation and sizing of synchronous condensers in weak grids with increased penetration of wind and solar farms," *IEEE J. Emerg. Sel. Topics Circuits Syst.*, vol. 11, no. 1, pp. 199–209, Mar. 2021.
- [118] D. Tzelepis, Q. Hong, C. Booth, P. N. Papadopoulos, J. Ramachandran, and G. Yang, "Enhancing short-circuit level and dynamic reactive power exchange in GB transmission networks under low inertia scenarios," in *Proc. Int. Conf. Smart Energy Syst. Technol. (SEST)*, Sep. 2019, pp. 1–6.
- [119] M. Yu, A. J. Roscoe, A. Dysko, C. D. Booth, R. Ierna, J. Zhu, and H. Urdal, "Instantaneous penetration level limits of non-synchronous devices in the British power system," *IET Renew. Power Gener.*, vol. 11, no. 8, pp. 1211–1217, Jun. 2017.
- [120] A. Kazerooni, S. Jupe, J. Berry, and N. Murdoch, "Sensitivity analysis of fault level assessments in HV networks," in *Proc. CIGRE Workshop*, 2014, pp. 1–5.
- [121] (2020). *System Strength in the NEM Explained*. [Online]. Available: <https://aemo.com.au/>
- [122] (2017). *Integrating Inverter Based Resources Into Low Short Circuit Strength Systems*. [Online]. Available: [https://www.nerc.com/comm/RSTC\\_Reliability\\_Guidelines/Item\\_4a\\_Integrating%20InverterBased\\_Resources\\_into\\_Low\\_Short\\_Circuit\\_Strength\\_Systems\\_-\\_2017-11-08-FINAL.pdf](https://www.nerc.com/comm/RSTC_Reliability_Guidelines/Item_4a_Integrating%20InverterBased_Resources_into_Low_Short_Circuit_Strength_Systems_-_2017-11-08-FINAL.pdf).
- [123] National Grid ESO. (2018). *System Operability Framework: Impact of Declining Short Circuit Levels*. [Online]. Available: <https://www.nationalgrideso.com/document/135561/download>.
- [124] National Grid ESO. (2022). *Provision of Short Circuit Level Data*. [Online]. Available: <https://www.nationalgrideso.com/document/135561/download>.
- [125] (2019). *Notice of Victorian Fault Level Shortfall At Red Cliffs*. [Online]. Available: [https://www.aemo.com.au/-/media/Files/Electricity/NEM/Security\\_and\\_Reliability/System-Security-Market-Frameworks-Review/2019/Notice\\_of\\_Victorian\\_Fault\\_Level\\_Shortfall\\_at\\_Red\\_Cliffs.pdf](https://www.aemo.com.au/-/media/Files/Electricity/NEM/Security_and_Reliability/System-Security-Market-Frameworks-Review/2019/Notice_of_Victorian_Fault_Level_Shortfall_at_Red_Cliffs.pdf)
- [126] R. Ierna et al., "Effects of VSM convertor control on penetration limits of non-synchronous generation in the GB power system," in *Proc. 15th Wind Integr. Workshop*, 2016.
- [127] A. Haddadi, E. Farantatos, I. Kocar, and U. Karaagac, "Impact of inverter based resources on system protection," *Energies*, vol. 14, no. 4, p. 1050, Feb. 2021.
- [128] M. Kuflo, P. Crossley, and M. Osborne, "Impact of 'intermediate' sources on distance protection of transmission lines," *J. Eng.*, vol. 2018, no. 15, pp. 913–917, Oct. 2018.
- [129] K. Jia, C. Gu, Z. Xuan, L. Li, and Y. Lin, "Fault characteristics analysis and line protection design within a large-scale photovoltaic power plant," *IEEE Trans. Smart Grid*, vol. 9, no. 5, pp. 4099–4108, Sep. 2018.

- [130] (2015). *System Operability Framework*. [Online]. Available: <https://www.nationalgrid.com/sites/default/files/documents/44046-SOF%202015%20Full%20Document.pdf>
- [131] B. J. Cory, B. M. Weedy, N. Jenkins, J. Ekanayake, and G. Strbac, *Electric Power Systems*. Hoboken, NJ, USA: Wiley, 2012.
- [132] S. I. Ocean, K. Cantley, and E. Hossain, "Quantifying power system strength to identify unique credible contingencies in renewable-dominated power systems," *Int. J. Electr. Power Energy Syst.*, vol. 172, Nov. 2025, Art. no. 111271.
- [133] L. Zhang, L. Harnfors, and H.-P. Nee, "Interconnection of two very weak AC systems by VSC-HVDC links using power-synchronization control," *IEEE Trans. Power Syst.*, vol. 26, no. 1, pp. 344–355, Feb. 2011.
- [134] E. Rahimi, A. M. Gole, J. B. Davies, I. T. Fernando, and K. L. Kent, "Commutation failure analysis in multi-infeed HVDC systems," *IEEE Trans. Power Del.*, vol. 26, no. 1, pp. 378–384, Jan. 2011.
- [135] M. H. Nawir, "Integration of wind farms into weak AC grids," Ph.D. dissertation, Cardiff Univ., Cardiff, U.K., 2017.
- [136] J. Z. Zhou, H. Ding, S. Fan, Y. Zhang, and A. M. Gole, "Impact of short-circuit ratio and phase-locked-loop parameters on the small-signal behavior of a VSC-HVDC converter," *IEEE Trans. Power Del.*, vol. 29, no. 5, pp. 2287–2296, Oct. 2014.
- [137] L. Huang, H. Xin, W. Dong, and F. Dörfler, "Impacts of grid structure on PLL-synchronization stability of converter-integrated power systems," *IFAC-PapersOnLine*, vol. 55, no. 13, pp. 264–269, 2022.



**RAFAT ALJARRAH** (Member, IEEE) received the Ph.D. degree in electrical and electronics engineering from The University of Manchester with power system engineering as a research subject. Also, he was awarded postgraduate certificates in the field of power systems and renewable energy (smart grids and sustainable electricity systems, analysis of electrical power and energy conversion systems, power system operation and economics, and solar energy technologies). He is currently an

Associate Professor of electrical engineering with Princess Sumaya University for Technology (PSUT). His research interests include future power systems, fault level monitoring, renewable energy, artificial intelligence, and power system protection.



**MAZAHER KARIMI** (Senior Member, IEEE) received the Ph.D. degree in power system engineering from the University of Malaya, in 2013. He has been an Associate Professor with the School of Technology and Innovations, University of Vaasa, Finland, since 2023. He has authored more than 100 peer-reviewed journal and conference papers, one book, three book chapters, and holds a co-inventor patent. His research interests

include substation automation, wide-area monitoring, protection and control of power systems, smart grid applications, distributed generation, energy management systems, and power system stability and frequency control, with a particular focus on grids supplied by renewable energy resources. He serves as a Guest Editor for IEEE TRANSACTIONS ON CONSUMER ELECTRONICS, *Energies*, and *IET Smart Grid*, and contributes to Working Group B5.57 on frequency protection challenges of CIGRE.



**HESAMODDIN MARZOOGHI** (Member, IEEE) received the bachelor's and master's degrees (Hons.) in electrical engineering (power) from Shiraz University, Shiraz, Iran, in 2009 and 2011, respectively, and the Ph.D. degree in electrical engineering (power) from The University of Sydney, Sydney, NSW, Australia, in 2016. He is currently the Director of Strategic Network Solutions Pty Ltd. His research interests are directed to stability analysis and control of power systems

with high penetration of renewable energy sources, distributed generation and energy storage, planning of future grids, and applications of intelligent systems in power engineering.

...